NASA CR-54428
MRB 5009Q1

Quarterly Report No. 1

STUDY OF FUEL CELLS USING STORABLE ROCKET PROPELLANTS

18 February to 17 May 1965

by

R. F. Drake, L. F. Athearn, R. E. Chute,
B. M. Fabuss, J. C. Orth, P. L. Terry, and J. O. Smith

prepared for

NATIONAL AERONAUTICS AND SPACE ADMINISTRATION

CONTRACT NAS3-6476

MONSANTO RESEARCH CORPORATION
BOSTON LABORATORY
Everett, Massachusetts 02149
Tel: 617-389-0480

NOTICES

This report was prepared as an account of Government-sponsored work. Neither the United States nor the National Aeronautics and Space Administration (NASA), nor any person acting on behalf of NASA:

A) Makes any warranty or representation, expressed or implied, with respect to the accuracy, completeness, or usefulness of the information contained in this report, or that the use of any information, apparatus, method, or process disclosed in this report may not infringe privately owned rights; or

B) Assumes any liabilities with respect to the use of, or for damages resulting from the use of any information, apparatus, method or process disclosed in this report.

As used above, "person acting on behalf of NASA" includes any employee or contractor of NASA, or employee of such contractor, to the extent that such employee or contractor of NASA, or employee of such contractor prepares, disseminates, or provides access to, any information pursuant to this employment with such contractor.

Dissemination outside the contracting government agency or to recipients other than Government defense contractors not authorized.

Request copies of this report should be referred to:

National Aeronautics and Space Administration
Office of Scientific and Technical Information
Washington, D. C., 20025
Attention: AFSS-A

NASA CR- 54428
MRB5009Q1

Quarterly Report No. 1

STUDY OF FUEL CELLS USING STORABLE ROCKET PROPELLANTS

18 February to 17 May 1965

by

R. F. Drake, L. F. Athearn, R. E. Chute,
B. M. Fabuss, J. C. Orth, P. L. Terry, and J. O. Smith

prepared for

NATIONAL AERONAUTICS AND SPACE ADMINISTRATION

28 May 1965

CONTRACT NAS3-6476

Technical Management
NASA Lewis Research Center
Cleveland, Ohio
Space Power Systems Division
Robert B. King, Technical Manager

MONSANTO RESEARCH CORPORATION
BOSTON LABORATORY
Everett, Massachusetts 02149
Tel: 617-389-0480

SUMMARY

This quarter we completed the design and construction of equipment to perform studies on (1) the decomposition of N_2O_4 to an oxygen-rich fuel cell feed stream, and (2) the decomposition or steam reforming of Aerozine-50 to a hydrogen-rich fuel cell feed stream.

Initial studies indicate that the N_2H_4 fraction of Aerozine-50 can be decomposed at moderate temperatures (about 80°C) with either a Rh or Raney Ni catalyst, but there is little decomposition of the UDMH (unsymmetrical dimethyl hydrazine). At 500°C a significant amount of thermal decomposition of UDMH was realized. Steam reforming of UDMH was accomplished with a Ni-base reforming catalyst at 500°C with an available H_2 efficiency of 37.4%.

There was little decomposition of N_2O_4 on 6 different catalysts with temperatures up to 800°C. The decomposition of NO demonstrated on some of these catalysts indicated an inhibiting effect in the N_2O_4 decomposition reaction either by N_2O_4 itself or by product O_2.

Studies on the direct use of N_2O_4 at MRD carbon cathodes indicate that carbon content and screen mesh size are important performance parameters. A method was developed to determine the diffusion rate of N_2O_4 through these electrodes. Diffusion rates were several times higher than stoichiometric requirements up to 200 ma/cm², indicating that excess reactant can dissolve in the electrolyte.

A catalyst program for the direct use of Aerozine-50 fuel produced at least one catalyst (Rh) that shows good activity. However, there is evidence that only the N_2H_4 component is active.

Design studies on 1/3 ft² electrodes for the direct use of N_2O_4 showed the importance of gas velocity and manifold grooving configuration on electrode performance. The water-removal problem has been attacked. Detailed data were acquired on the transport of water vapor through the electrodes. The electrode and manifold geometry for 1/3 ft² N_2O_4 electrodes has been established.

TABLE OF CONTENTS

TABLE OF CONTENTS (Continued)

LIST OF FIGURES

LIST OF FIGURES (Continued)

LIST OF TABLES

LIST OF TABLES (Continued)

I. INTRODUCTION

A. BACKGROUND

This is the third stage of an investigation whose objective is to develop a fuel cell operating on storable rocket propellants as primary or secondary reactants. Work on the previous contract (NAS3-4175) largely concerned the investigation of a number of possible systems and cell configurations and culminated in the construction and long-term testing of two cell types. One configuration used N_2H_4 dissolved in KOH electrolyte as the fuel and gaseous O_2 as the oxidizer. The other system used N_2H_4 dissolved in H_3PO_4 electrolyte as the fuel and gaseous N_2O_4 as the oxidizer. Both systems were developed to the point where System Designs were submitted to NASA specifications (Ref. 1).

The present contract calls for the investigation and development of cells operating on gaseous N_2O_4 and Aerozine-50 as direct reactants, and for a reforming capability to use these reactants to produce O_2- and H_2-rich feedstreams for fuel cells. The construction and operation of working reformers and cells are the objectives of this work.

B. PROGRAM ORGANIZATION

The project consists of three phases, to be performed roughly in series. The overall work plan shown in Figure 1 illustrates the major tasks to be performed. Detailed working plans for Phase I have been developed and are illustrated in Figure 2. There are three major tasks in this phase: reforming of Aerozine-50, catalytic decomposition of N_2O_4, and electrode development for direct reactant use. Each task has been further broken down into subtasks which represent the actual work being done to complete the task successfully. Subtasks are discussed in more detail in Appendix I.

The project and this report have been organized around the task-subtask and PERT concepts. The advantages of this arrangement are:

1. It insures adequate planning.
2. It aids clarity of communication.
3. It gives a clear picture of project status.
4. It pinpoints problem areas and trouble spots early.

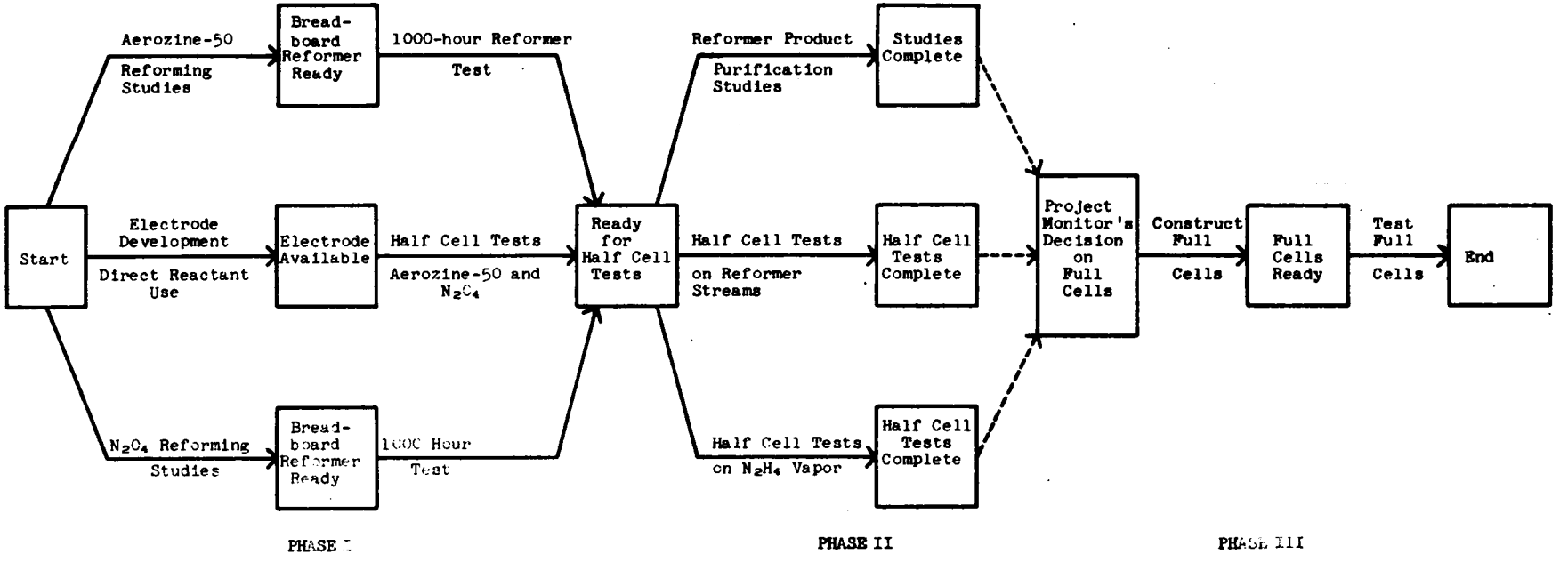

Figure 1. PROGRAM WORK PLAN AND EVENT CHART
NAS3-6476

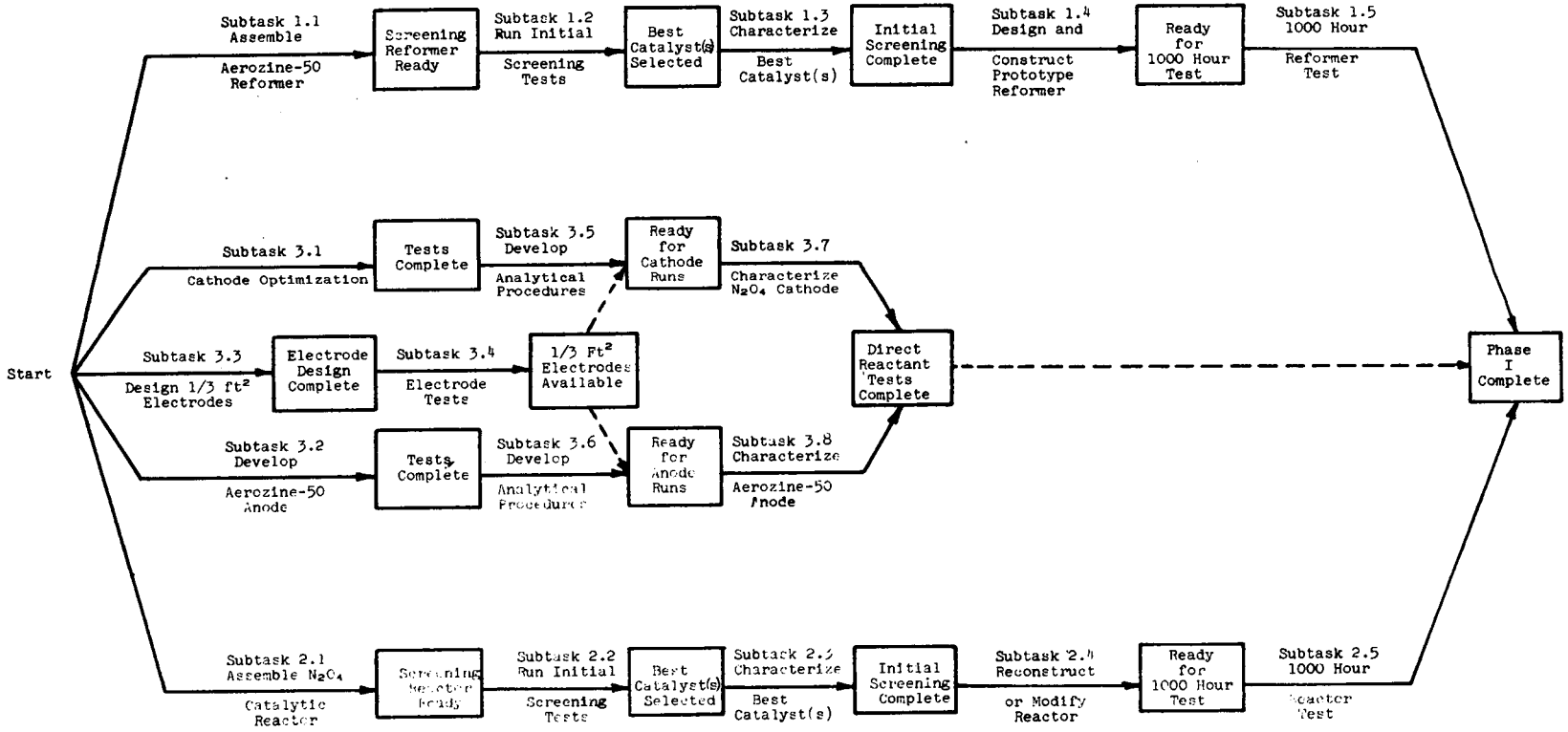

PERT CHART

Figure 2. NAS3-6476 Phase I

C. SCOPE OF THIS REPORT

This report covers work done on the subtasks listed below (refer to Figure 2 and Appendix I).

Subtask Number	Description	Work Status
1.1	Assemble Aerozine-50 Reformer	complete
1.2	Run Initial Screening Tests	40% complete
2.1	Assemble N_2O_4 Catalytic Reactor	complete
2.2	Run Initial Screening Tests	25% complete
3.1	Cathode Optimization	50% complete
3.2	Develop Aerozine-50 Anode	25% complete
3.3	Design 1/3-ft^2 Electrodes	50% complete

II. TASK I. REFORMING OF AEROZINE-50

A. BACKGROUND

1. Objectives

a. Low-Temperature Decomposition

The objective of this subtask is to produce a hydrogen-rich (over 50%) gas product stream utilizing as much of the available hydrogen as possible.

b. High-Temperature Reforming

The objective of this subtask is to use potential H_2 from the UDMH portion of Aerozine-50 by steam reforming, thus giving greater H_2 output per pound of Aerozine-50 input.

2. Literature

a. Low-Temperature N_2H_4 Decomposition

Low-temperature N_2H_4 decomposition was investigated by Audrieth and Jolly (Ref. 2) with Raney nickel catalyst, both with and without platinum promoters. The temperature range investigated was 0-50°C, over which an activation energy of 17.1 kcal/mole was found. The decomposition yielded H_2, N_2 and NH_3, with about 75-83% of the N_2H_4 decomposing H_2 and N_2. At 25°C, with unpromoted Raney nickel catalyst, gas evolution rates of 8.4 ml per min. per g catalyst was obtained, while Raney nickel with 13% K_2PtCl_6 promotion gave a rate of 100.0 ml of gas/min./g catalyst.

Russian workers (Ref. 3) investigating the catalytic activity of polychelates on N_2H_4 vapor at 74°C and 104°C found that some copper and zinc polychelates gave over 80% reaction to H_2 and N_2, while a cobalt polychelate gave NH_3 almost completely. The catalysts were the most specific found; others producing N_2, H_2 and NH_3 were also tested.

A German patent (Ref. 4) assigned to Engelhard Industries, Inc., disclosed hydrazine decomposition catalysts. No numerical data are given, but the following general comments are noted:

0.5% Rhodium on alumina gave high gas evolution with very little NH_3 (as determined by odor).

0.5% Iridium on alumina yielded a lower gas rate and also very little NH_3 odor.

0.5% Pt on alumina gave a low gassing rate and low NH_3 odor.

5.0% Rhodium on alumina yielded very little gas evolution.

b. High-Temperature N_2H_4 Decomposition

Thermal decomposition (noncatalytic) was studied by H. W. Lucien (Ref. 5) at 175-250°C and 300-430 psig. The following trends were noted:

Trace amounts of NH_3 (<2%) inhibited N_2H_4 decomposition; over 2% gave no further change.

Decomposition rate decreased with increasing pressure.

Activation energy was 72.7 kcal/mole.

Higher pressures increased per cent H_2 at equilibrium; however, the percentage was very small at all pressures. At 300 psig the N_2/H_2 ratio was 15, while at 430 psig the N_2/H_2 ratio was 4.5. The best value corresponds to only 4% decomposition by the H_2 plus N_2 route.

Higher temperatures give higher per cent H_2 at equilibrium. At 222°C the N_2/H_2 ratio was 12, while at 250°C the ratio was 5 (both at 400 psig).

All attempts to decompose N_2H_4 at less than 10 psig in the confined system resulted in explosions.

Heterogeneous thermal decomposition on a silica vessel was investigated by Hanratty, et al (Ref. 6) at 300-700°C at nearly atmospheric pressure in a flow reactor.

The reaction was found to be a first-order heterogeneous decomposition between temperature limits studied. Activation energies were 9-16 kcal/mole. Only 6% H_2 was found in gas effluent, increasing with temperature.

c. High-Temperature UDMH Decomposition

Catalytic decomposition of 1,1-dimethyl hydrazine was tested on a number of catalysts by Engelhard Industries, Inc. (Ref. 7). This was done in the vapor state diluted with either H_2, N_2, or He carrier gas at temperatures ranging from 100 to 350°C. Data are given in terms of CH_4-to-N_2 ratio. The lower this ratio, the more H_2 was produced. The best catalysts for H_2 production were rhodium and iridium on various supports. In general, higher temperatures produced more H_2. The poorest catalysts for H_2 production were palladium and ruthenium.

Thermal decomposition of UDMH in a flow reactor (noncatalytic) was studied by H. F. Cordes (Ref. 8), at 400°C. A first-order homogeneous reaction was found. The primary product at 250°C was CH_4. The H_2 quickly formed a low steady state concentration and did not vary with residence time. At the higher temperatures

ethane and propane were found, indicating a chain reaction propagated through $CH_3\cdot$ radicals. An activation energy of 28.7 kcal/mole was found.

d. High-Temperature UDMH Steam Reforming

This method of UDMH reforming was tested in a preliminary manner under the previous contract (Ref. 1). At 300°C, after passing through four catalyst beds containing Pd, Pt, Rh and Ru, the gas composition was: 19% H_2, 11% N_2, 11% CO, 15% CH_4, 3% C_2H_6 and 42% NH_3.

This demonstrates the good potential of the steam-reforming approach.

3. Discussion of Theory and Reactions

The reforming of Aerozine-50 can be discussed in two temperature ranges: (1) high temperature reforming (above 200°C); and (2) low temperature reforming (50-200°C).

These two categories can further be broken down with reference to the two components of Aerozine-50, namely, N_2H_4 and UDMH. UDMH can further be discussed with respect to decomposition and steam reforming.

Experimentally, it is simpler to evaluate each component separately before investigating the more involved mixtures. It is believed that data so obtained can be integrated to reasonably predict the behavior of Aerozine-50.

a. Low-Temperature N_2H_4 Decomposition

There are two possible reaction paths for N_2H_4 decomposition in general. Both of these are integrated into the following equation:

$$(3 + x)N_2H_4 \longrightarrow 4\ NH_3 + (1 + x)N_2 + 2x\ H_2 \qquad (1)$$

where x = number of moles of N_2H_4 converted to $N_2 + H_2$ per 3 moles N_2H_4 converted to NH_3.

Experimentally, the NH_3 is absorbed in H_2SO_4. The H_2/N_2 ratio is then determined by VPC and x can be determined from the equation: $2x/1+x = H_2/N_2$. The per cent N_2H_4 reacting to give $N_2 + H_2$ is $100x/3+x$. Thus, a very high value of x indicates high hydrogen production, and x can range from 0 to ∞.

The reaction products at low temperatures are determined entirely by specific catalyst interactions, some catalysts producing mostly NH_3 and others 80-90% H_2 plus N_2.

If the N_2H_4 in Aerozine-50 were completely decomposed to H_2 plus N_2, while the UDMH is not affected, a hydrogen-rich gas would be produced (67% H_2 - 33% N_2). It could be immediately used in a fuel cell, and 48% of the available input hydrogen would be recovered for use. This would be a very simple system, since no heat would be needed. Rather, cooling might be necessary since ΔH at 25°C for 1 mole of N_2H_4 producing $2H_2$ plus N_2 is -22.75 kcal. This system would undoubtedly be the most efficient from an overall energy standpoint since no energy would be needed for heating. This method has high possibility of successful operation. Table 1 shows the relative merits of a number of possible high- and low-temperature systems with Aerozine-50.

b. High-Temperature N_2H_4 Decomposition

Difficulties might be encountered at higher temperatures owing to greater NH_3 formation with thermal, noncatalytic N_2H_4 decomposition. This will have to be determined from experimentation. One method to overcome this problem might be to use two reactor zones, one at low temperatures for N_2H_4 decomposition, and another at higher temperatures for UDMH reforming.

c. UDMH Decomposition

It is unlikely that anything but CH_4 and N_2 will be produced from UDMH decomposition at low temperatures although reference 7 suggests some specific catalysts that might produce some H_2. However, data on relative bond strengths show the following.

Bond	Strength, kcal/mole	Reference
$H—N_2H_3$	93 (newest value)	9
$H—NH_2$	103	9
$H—CH_3$	104	9
$H—C_2H_5$	98.3	9
$H—NHCH_3$	91	9
N—N (for UDMH)	60	1 and 10
C—N (for UDMH)	80	1 and 11

Table 1

POSSIBLE REFORMING OUTPUTS OF AEROZINE-50

No.	Reactions Assumed	Feed Composition, mole-%	Moles H_2 per 100 g Feed	Product Gas Composition, mole-%	Hydrogen Efficiency H_2 Out/H_2 In, %	Notes on System Limitations and Strong Points
1	Only N_2H_4 decomposed $N_2H_4 \longrightarrow H_2 + 2H_2$	N_2H_4 65.3 UDMH 34.7	3.12	H_2 56.6 N_2 28.3 UDMH 15.1	48.4	At low temperatures, ambient to 50°C. Simplified systems requirements, liquid system.
2	$N_2H_4 \longrightarrow N_2 + 2H_2$ UDMH $\longrightarrow 2CH_4 + N_2$	N_2H_4 65.3 UDMH 34.7	3.12	H_2 43.5 N_2 33.3 CH_4 23.2	48.4	Medium temperature at vapor pressure of Aerozine. Product H_2 diluted with CH_4 still usable in fuel cell.
3	$N_2H_4 \longrightarrow N_2 + 2H_2$ UDMH $\longrightarrow C_2H_6 + N_2 + H_2$	N_2H_4 65.3 UDMH 34.7	3.95	H_2 55.1 N_2 33.3 C_2H_6 11.6	61.2	Temperature range 300-500°C might be possible, high H_2 composition might be directly usable in fuel cell.
4	$N_2H_4 \longrightarrow N_2 + 2H_2$ UDMH $\longrightarrow 2C + N_2 + 4H_2$	N_2H_4 65.3 UDMH 34.7	6.44	H_2 73.0 N_2 27.0	100	Possible in 300-500°C, temperature range. Carbon deposition may severely limit catalyst life. Gas stream directly usable in fuel cell.
5	$N_2H_4 \longrightarrow N_2 + 2H_2$ 50% UDMH $\longrightarrow CO_2$ 50% UDMH unreacted UDMH + $4H_2O \longrightarrow 2CO_2 + N_2 + 8H_2$	N_2H_4 17.3 UDMH 9.2 H_2O 73.5	2.93	H_2 44.0 N_2 13.5 CO_2 5.7 H_2O 34.0 UDMH 2.8	19.8‡	Input H_2O/C ratio = 4 moles H_2O/g-atom of carbon nonequilibrium conditions, possible at 300-500°C, output directly usable.
6	$N_2H_4 \longrightarrow N_2 + 2H_2$ 40% UDMH $\longrightarrow CO_2$ 40% UDMH $\longrightarrow$ CO 20% UDMH $\longrightarrow CH_4$	N_2H_4 17.3 UDMH 9.2 H_2O 73.5	3.53	H_2 47.2 N_2 14.5 CO_2 4.0 H_2O 28.3 CO 4.0 CH_4 2.0	23.9‡	Near equilibrium conditions in 500-700°C range, dirty gas containing 4.0% CO, may be directly usable in fuel cell. Input H_2O/C ratio = 4:1 (see 5 above).
7	$N_2H_4 \longrightarrow N_2 + 2H_2$ 100% UDMH to CO UDMH + $2H_2O \longrightarrow 2CO + N_2 + 6H_2$	N_2H_4 17.3 UDMH 9.2 H_2O 73.5	3.68	H_2 47.3 N_2 14.0 CO 9.7 H_2O 29.1	24.8‡	Equilibrium conditions at 700°C or higher. Dirty gas, 9.7% CO could not be directly used in fuel cell. Input H_2O/C ratio = 4:1 (see 5 above).

‡ Includes H_2 from H_2O.

It can be seen that the N—N bond is the weakest, and that the second weakest is the C—N bond. It thus seems probable that the catalyst will align molecules in such a way as to produce primarily CH_4 and N_2 for heterogeneous reactions. For thermal cracking, amines and CH_4 seem very likely, with propane and ethane formed at higher temperatures, where $CH_3\cdot$ radicals are more stable (Ref.8).

Thus the main hope in UDMH decomposition lies with specific catalysts that may produce carbon deposition (mentioned in Ref. 7). Medium temperatures, 200-400°C, should be best for H_2 production.

d. UDMH Steam Reforming

There are five reactions that must be considered in steam reforming UDMH:

$$(CH_3)_2NNH_2 + 4H_2O \longrightarrow 2CO_2 + N_2 + 8H_2 \quad (2)$$

$$(CH_3)_2NNH_2 + 4H_2O \longrightarrow 2CO_2 + 2NH_3 + 5H_2 \quad (3)$$

$$(CH_3)_2NNH_2 + 2H_2O \longrightarrow 2CO + N_2 + 6H_2 \quad (4)$$

$$(CH_3)_2NNH_2 + 2H_2O \longrightarrow 2CO + 2NH_3 + 3H_2 \quad (5)$$

$$(CH_3)_2NNH_2 \longrightarrow 2CH_4 + N_2 \quad (6)$$

ΔF for these reactions = ΔF_f products - ΔF_f reactants.

While the value of ΔF_f of UDMH is not known at the temperatures where these reactions will proceed, the relationship between these reactions can be seen by defining ΔF_f of UDMH as a constant C at each temperature. This gives a value of $\Delta F + C$ for the reactions as shown in Table 2.

In all reactions, the complete removal of UDMH at equilibrium will be favored since C will be much more positive than the sum of the other ΔF_f terms.

Equilibrium conditions would produce large amounts of CH_4 and N_2 at the lower temperatures, and this effect would decrease with temperature increase. However, even at 527°C, CH_4 formation will be a significant factor at equilibrium.

NH_3 formation is significant at 227°C with respect to reforming. However, at the higher temperatures very little NH_3 should be present.

At 527°C, CO + CO_2 formation are both significant. At lower temperatures CO_2 is favored and at higher temperatures (>700°C) CO is favored.

Table 2

FREE ENERGY RELATIONSHIPS ($\Delta F + C$) OF POSSIBLE REFORMING REACTIONS

Reaction Number	($\Delta F + C$) in kcal/mole			
	227°C	327°C	427°C	527°C
2	20.64	15.72	10.66	5.48
3	22.86	23.28	23.68	24.06
4	30.44	23.70	16.90	10.08
5	32.66	31.26	29.92	28.66
6	-15.70	-10.98	- 6.10	- 1.06

* At 90°C ΔF_f of UDMH = 56.2 kcal/mole and is increasing in a positive direction.

Thus, to produce significant H_2 in the temperature range 200-400°C, a nonequilibrium situation must exist. This is made possible by using catalysts that have slow rates for the reaction

$$4H_2 + CO_2 \longrightarrow 2H_2O + CH_4 \qquad (7)$$

which is normally slow at low temperatures, allowing commercial reforming units to shift CO to CO_2.

To reach a high H_2 conversion under equilibrium conditions, it would be necessary to operate around 700°C to lower the CH_4 content of the gas. At this temperature mainly CO rather than CO_2 would be present.

Carbon deposition cannot occur at equilibrium with the H_2O/C ratio being considered; however, in nonequilibrium situations this might be significant.

e. Approach

Table 1 lists the types of reactions for Aerozine-50 that we consider most promising. Each of the seven systems has favorable aspects concerning one or more of the following: H_2 per 100 g input Aerozine 50, H_2 per 100 g total input, H_2% in gas

composition, H_2 efficiency, direct use of output gas, energy efficiency, and development simplicity.

We must determine first which system can be approached experimentally, and then choose the best overall system.

To do this we will study first the decomposition of N_2H_4 and UDMH separately to find catalysts and conditions that will be satisfactory for each. If either component cannot be utilized in a particular system, that system will be eliminated.

When a system is found in which both components of Aerozine-50 perform satisfactorily, we can then integrate into a complete system with more detailed knowledge than if Aerozine-50 had been tested as a mixture.

B. RESULTS AND DISCUSSION

1. Equipment and System

a. Low-Temperature Testing

Figure 3 shows a schematic diagram of the experimental setup used for most of the tests. Figure 4 is a photograph of the system. A thermostatted water bath was heated by a copper coil heater controlled by Thermistemp temperature regulator (± 0.1°C). The reactor flask was a 50-ml round-bottomed flask, with a magnetic stirring bar enclosed. An addition funnel was used to add the fuel instantly or in small increments. From the flask a gas exit line vented to a manometer used to check for pressure leaks, and to a sulfuric acid scrubber for NH_3 removal. From the scrubber the gas passed through a gas sample calibration tube and then into a wet test meter for volume measurements.

The tests were conducted by adding a known weight and volume of catalyst to the reaction flask. The addition funnel was filled with the fuel to be tested, and the system was purged with N_2 to remove any air. The fuel was added dropwise to insure safe decomposition rates. When it was obvious that no explosive decompositions would occur, the remainder of the fuel was added and the gas evolution rate measurements were started. The gas sample was analyzed by VPC.

b. High-Temperature Testing

Figure 5 shows schematically the complete high-temperature reforming system, and Figure 6 is a photograph of the system. A calibrated one-liter graduate contains the water-fuel mixture, feeding into Milton Roy "mini-pump" (maximum pressure 200 psig), through a 5-micron s.s. filter. Immediately following the pump outlet is a pressure gauge and rupture disc assembly that will release at 200 psig. The pressure gauge permits the use of the pump calibration with pressure for accurate pumping rates.

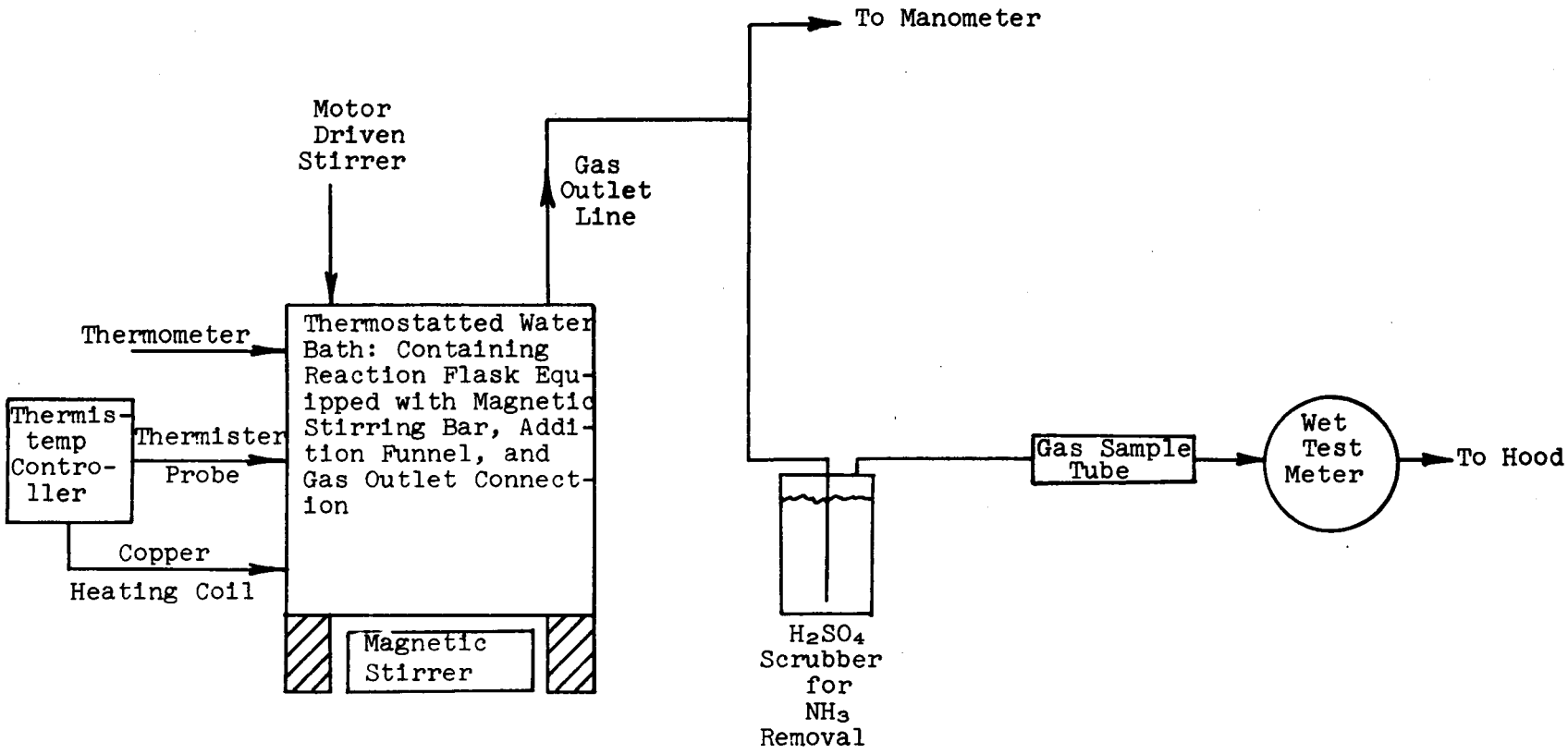

Figure 3. Low Temperature Decomposition Test Apparatus Schematic

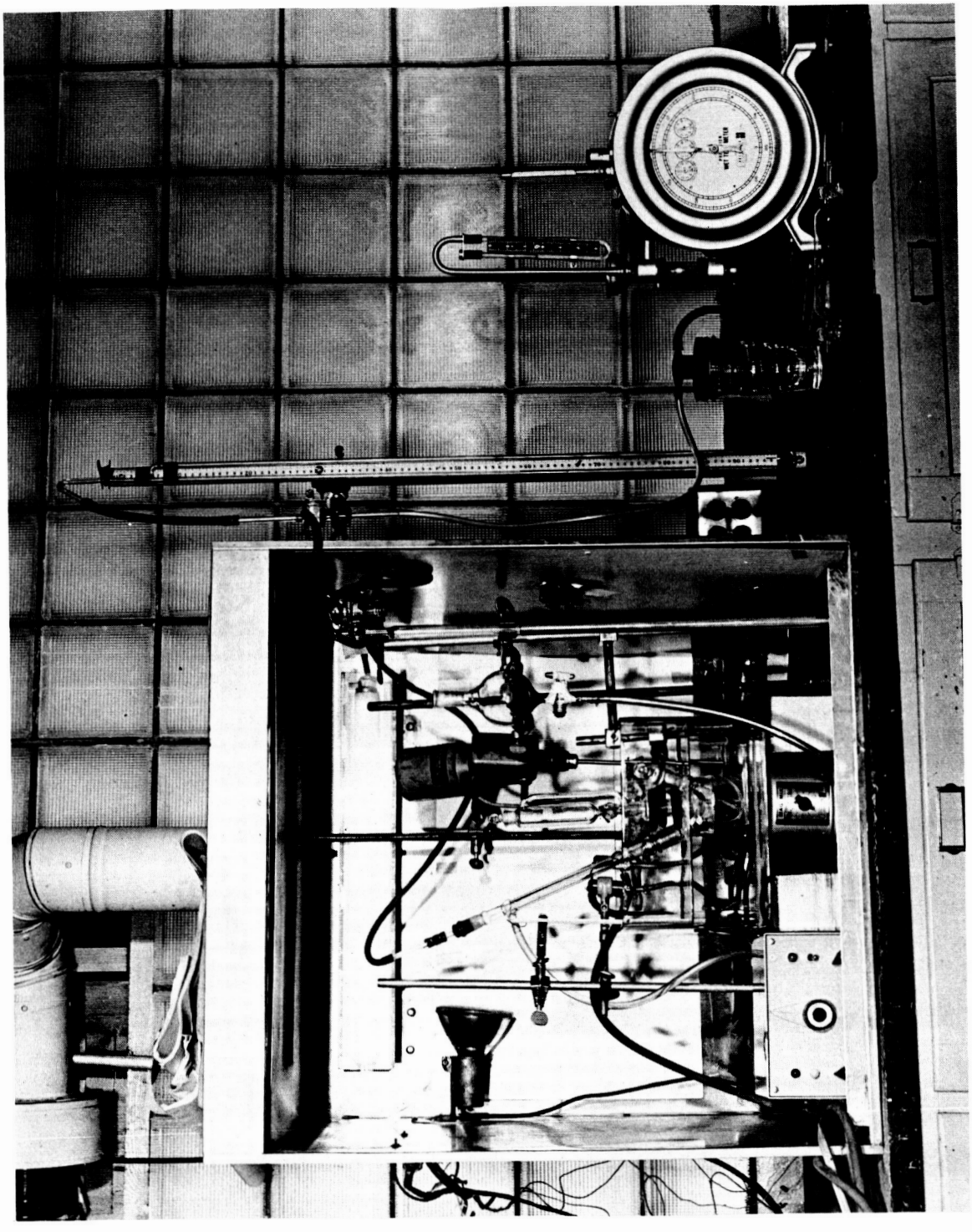

Figure 4. Photograph of Low Temperature Decomposition Test Apparatus

5009Q2

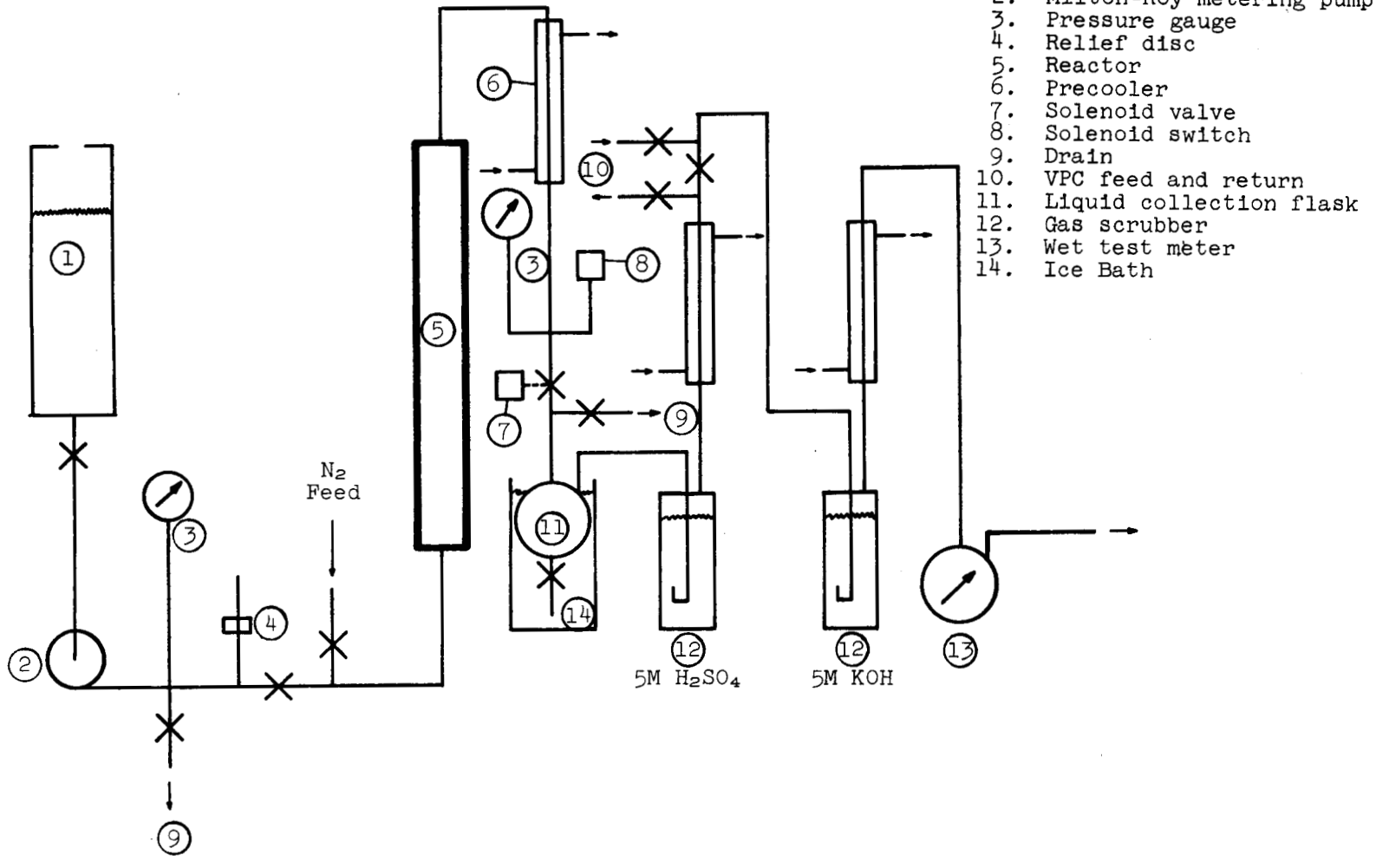

Figure 5. High-Temperature Reforming System Schematic

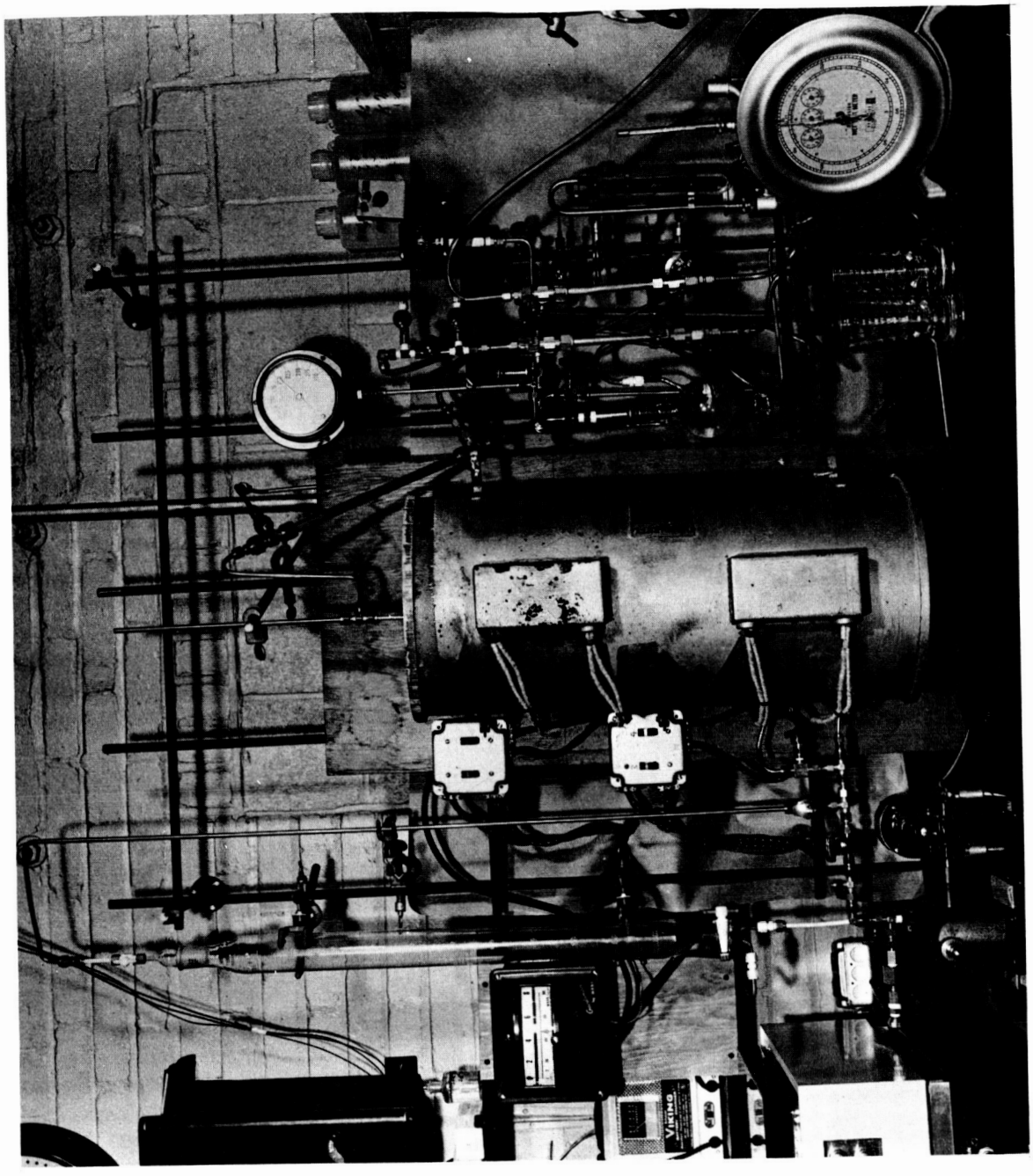

Figure 6. Photograph of High Temperature Reforming System

5009Q2

Following the rupture disc is a valve system to purge and clean the pump. A valved gas input line is used (argon or helium) to purge the system of air before testing and to purge the liquid and gases remaining after the test period. The reactor system, consisting of a 1-in. 304 s.s. pipe with 3/4-in. I.D. is heated by a 3400-watt electric oven, with individual on-off switches on four heating elements. Thermocouples are attached to the reaction tube and connect to a West temperature controller and a Brown temperature recorder. The output of the reactor goes through a water condenser to a manostat consisting of a pressure gauge and a pressure switch that activates an on-off solenoid valve, maintaining pressure within 5 psig. Following the solenoid valve is the liquid-gas separator flask, cooled in an ice bath to lower the vapor pressure of the exit liquids. The flask is partially filled with 5N H_2SO_4 (100 ml) to trap the unreacted Aerozine-50 along with NH_3, while passing CO_2. The gases then enter an H_2SO_4 scrubber to remove any trace of NH_3, flow through another condenser to a KOH trap to remove CO_2, and then flow to the wet test meter. In between the H_2SO_4 scrubber and the KOH scrubber is a valve to allow the gas to pass through the sample loop of a vapor phase chromatograph for analysis, and then back to the KOH scrubber. This permits gas analysis at any time during the test. After the wet test meter, the out gas is vented to a hood.

The reactor tube is 22 in. long and is packed with 10 in. of porcelain chips for preheating, then six inches of catalyst bed (43 ml volume), and then 4 more inches of porcelain chips.

The pump has been calibrated with water at different stroke settings, and system pressures as shown in Figures 7 and 8.

We have not yet successfully analyzed the liquid product trap for determination of UDMH, N_2H_4, and NH_3 together. However, we expect to solve this problem soon.

The VPC is now ready to be calibrated on the gases expected in the reformer output.

2. Experimental Results

a. Low-Temperature System

Table 3 shows the experimental data obtained with the low-temperature decomposition studies.

(1) UDMH Decomposition

Thus far, no catalysts have been found that give an effective low-temperature decomposition of UDMH in the liquid state. In all tests the decomposition stopped after a slow reaction for 20 to 30 minutes. This may indicate that only an impurity* in the UDMH is reacting.

* The UDMH used is labeled as 98-99% pure.

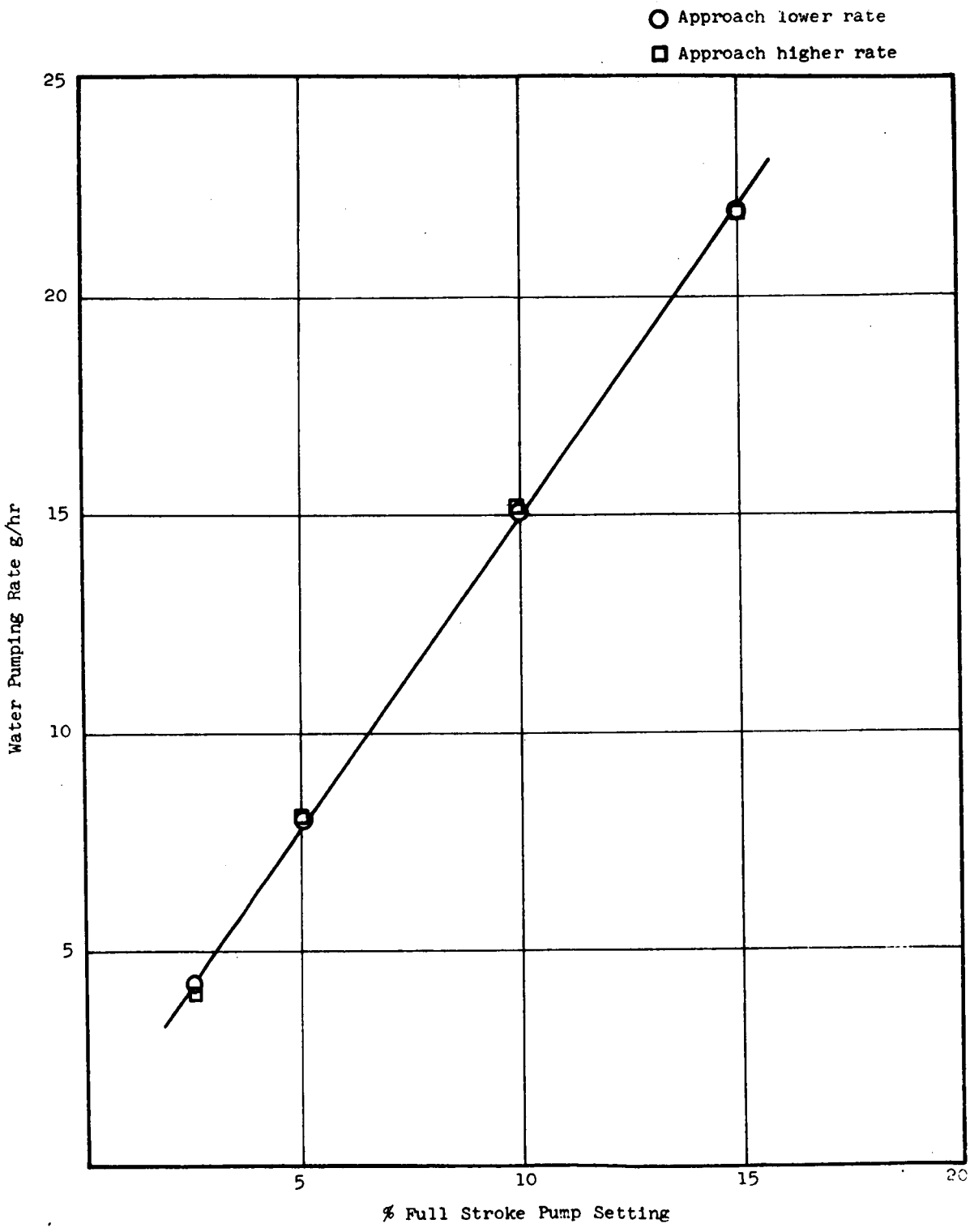

Figure 7. Calibration Curve for Metering Pump

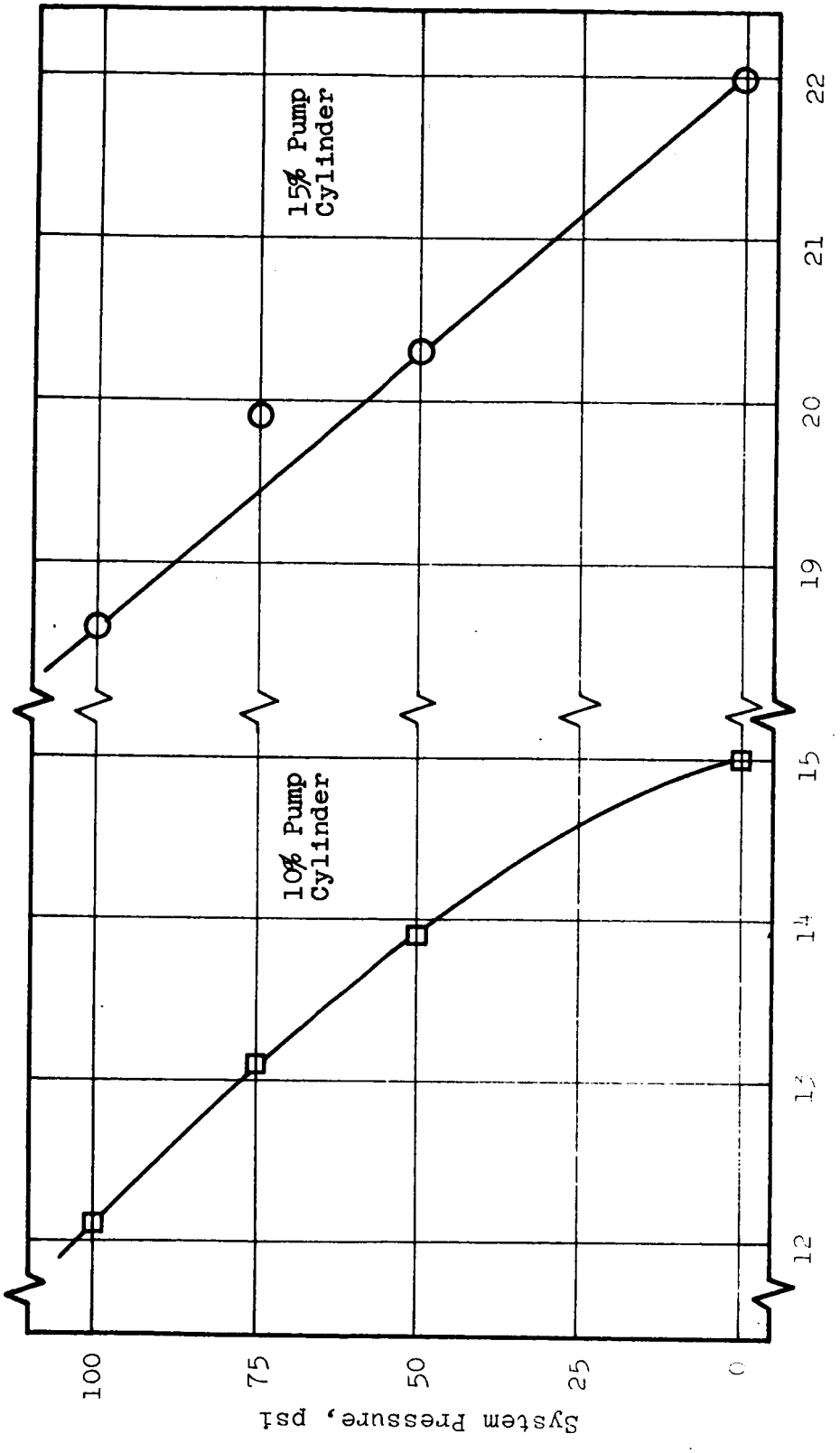

Figure 8. Calibration Curve for Metering Pump at Elevated Pressures

Table 3

LOW TEMPERATURE DECOMPOSITION OF N_2H_4, UDMH AND 50/50 MIXTURES

Catalyst	Catalyst Volume, ml	Catalyst Weight, g	Fuel	Temp, °C	Gas Rate, ml/min	Specific Gas Rate, ml/min-g*	Specific Gas Rate, ml/min-ml	H_2/N_2 Ratio	% N_2H_4 to H_2	Notes
Raney nickel water slurry no. 28, Raney Nickel Corp.	1	-	UDMH	30	1.0	-	1.0	-	-	same catalyst
	1	-	UDMH	61	0.2	-	0.2	-	-	
Raney nickel water slurry, with 0.3 g H_2PtCl_6	1	-	UDMH	61	0.2	-	0.2	-	-	fresh catalyst
	1	-	50/50	61	294	-	294	-	-	same catalyst
	1	-	UDMH	61	0.45	-	0.45	-	-	same catalyst
	1	-	25% N_2H_4 75% UDMH	59	225	-	225	-	-	same catalyst
	1	-	N_2H_4	34	560	-	560	1.90	88	fresh catalyst
Raney nickel-water slurry, no platinum	1	-	N_2H_4	24	21.4	-	21.4	-	-	fresh catalyst
	1	-	N_2H_4	26	28.3	-	28.3	-	-	same catalyst
Girdler T-242, Ni + Cu oxides, 1/8-in. tablets	3	2.25	UDMH	30	0.9	0.4	0.3	-	-	fresh catalyst
	3	2.25	50/50	30	negl.	-	-	-	-	same catalyst
Baker 0.5% Pt on alumina, 1/8-in. tablets	3	1.80	UDMH	30	1.4	0.8	0.5	-	-	rate decreasing with time
	3	1.80	50/50	30	0.6	0.3	0.2	-	-	
Girdler T-308, 0.05% Pd on act. alumina, 1/8-in.tablets.	3	2.2	UDMH	30	0	-	0	-	-	
	3	2.2	50/50	30	negl.	-	-	-	-	
Girdler G-60 promoted Ni catalyst, 3116 x 1/8 in. tablets	3	2.8	UDMH	30	1.1	0.4	0.4	-	-	rate decreasing with time
	3	2.8	50/50	30	negl.	-	-	-	-	
Girdler T-325 reduced stabilized nickel 1/8-in. tablets	3	2.3	N_2H_4	30	7.7	3.3	2.6	-	-	same catalyst
	3	2.3	50/50	30	8.2	3.6	2.7	-	-	rate decreasing,
	3	2.3	UDMH	30	0.6	0.3	0.2	-	-	fresh catalyst
	3	2.3	50/50	30	6.7	2.9	2.2	-	-	same catalyst, rate increasing

Table 3 (Continued)

Catalyst	Catalyst Volume, ml	Catalyst Weight, g	Fuel	Temp, °C	Gas Rate, ml/min	Specific Gas Rate, ml/min-g*	Specific Gas Rate, ml/min-ml	H_2/N_2 Ratio	% N_2H_4 to H_2	Notes
Girdler T-323 reduced stabilized cobalt 1/8-in. tablets	3	3.1	N_2H_4	30				-	-	Explosive decomposition
	1	1.0	UDMH	30	2.2	2.2	2.2	-	-	Decomposition stopped after 20 minutes.
	1	1.0	50/50	30	49.7	49.7	49.7	0.05	0.9	Trace CH_4 in gas sample
Girdler G-52 reduced stabilized Ni 37% on Al_2O_3	3	2.8	UDMH	30	1.1	0.4	0.4	-	-	Rate decreasing with time
	3	2.8	50/50	30	negl.	-	-	-	-	
Engelhard - 5% Rh on carbon powder	2.5	0.7	N_2H_4	29.9	18.6	26.6	7.4	1.56	54.5	
	2.5	0.7	UDMH	29.9	0.8	1.1	0.3	-	-	same catalyst, rate decreasing
	2.5	0.7	50/50	29.9	5.2	7.4	2.1	-	-	same catalyst
	2.5	0.7	50/50	34.6	8.8	12.6	3.5	-	-	same catalyst
	2.5	0.7	50/50	39.4	12.8	19.7	5.1	1.33	40	same catalyst
Baker 0.5% Rh on alumina	3	2.2	N_2H_4	29.9	2.8	1.3	0.9	1.56	55	
Proprietary catalyst on Pt mesh	-	0.7	N_2H_4	29.9	0.6	0.9	-	-	-	
	-	0.7	N_2H_4	39.5	3.3	4.7	-	-	-	
	-	0.7	N_2H_4	49.8	7.3	10.4	-	-	-	
	-	0.7	50/50	49.4	6.4	9.1	-	0.42	8	
	-	0.7	UDMH	49.5	0	0	-	-	-	
Engelhard Rhodium Black	-	0.1	N_2H_4	49.7	24.3	243	-	-	-	
	-	0.1	UDMH	49.7	0	0	-	-	-	
	-	0.2	50/50	50.0	27.2	136	-	-	-	

* Per gram of catalyst.

Note: In tests where gas evaluation rate was 30 ml/min or greater the reaction was allowed to go to completion. In these cases it was determined that all of the N_2H_4 decomposed to H_2, N_2 or NH_3 and none of the UDMH decomposed.

(2) N_2H_4 Decomposition

The best catalyst found for N_2H_4, both from a standpoint of H_2 production and high evolution rate, is a Raney nickel-water slurry (see Table 3) that has been promoted by addition of 0.3 g of H_2PtCl_6. However, this catalyst does not lend itself to higher temperature reactor systems.

The next best catalyst is a rhodium black catalyst, which exhibited a significantly high decomposition rate, but produced only 58% conversion to H_2, the rest reacting to form NH_3.

Other forms of rhodium catalysts such as 5% rhodium on carbon powder and 0.5% rhodium on alumina tablets were tested at lower temperatures. All forms of rhodium catalysts tested, if extrapolated and compared on weight-of-rhodium basis, yield equal gas evolution rates. All rhodium catalysts also produced 43-46% NH_3 from the N_2H_4 input.

A reduced cobalt catalyst, Girdler T-323, caused an explosive decomposition that might have been due to adsorbed oxygen. A fairly high decomposition rate was found with a proprietary MRC catalyst. However, both of these catalysts when later tested on 50/50 mixtures produced mostly NH_3 and very little H_2.

(3) 50/50 Mixtures

In general, the decomposition rates with 50/50 mixtures of the hydrazines showed a lower gas evolution rate than with pure N_2H_4, and also produced a larger amount of NH_3 (see Table 3). This finding agrees with the theory of N_2H_4 decomposition cited by reference 12, which predicts NH_3 and amines in general to have an inhibitory effect on N_2H_4 decomposition. However, in most cases the rate drops only by a factor of two. The reaction is still temperature dependent by the same amount as found by Audrieth, et al (Ref. 2), for N_2H_4 with Raney nickel catalysts. Figure 9 shows a plot of reaction rate as a function of the reciprocal of the absolute temperature for Engelhard 5% rhodium on carbon powder. The activation energy, 18 kcal/mole, agrees with that given in reference 2. This indicates that reaction is not diffusion controlled since changes in diffusion rates do not exhibit this type of temperature dependence.

b. Conclusions

(1) Fifty-fifty mixtures of N_2H_4 and UDMH may be used for H_2 production at low temperatures (30-80°C) in the liquid state. Only the N_2H_4 portion decomposes, yielding 60-90% of the available H_2 from the N_2H_4, depending on the catalyst. The rates are sufficiently high for practical consideration in this application.

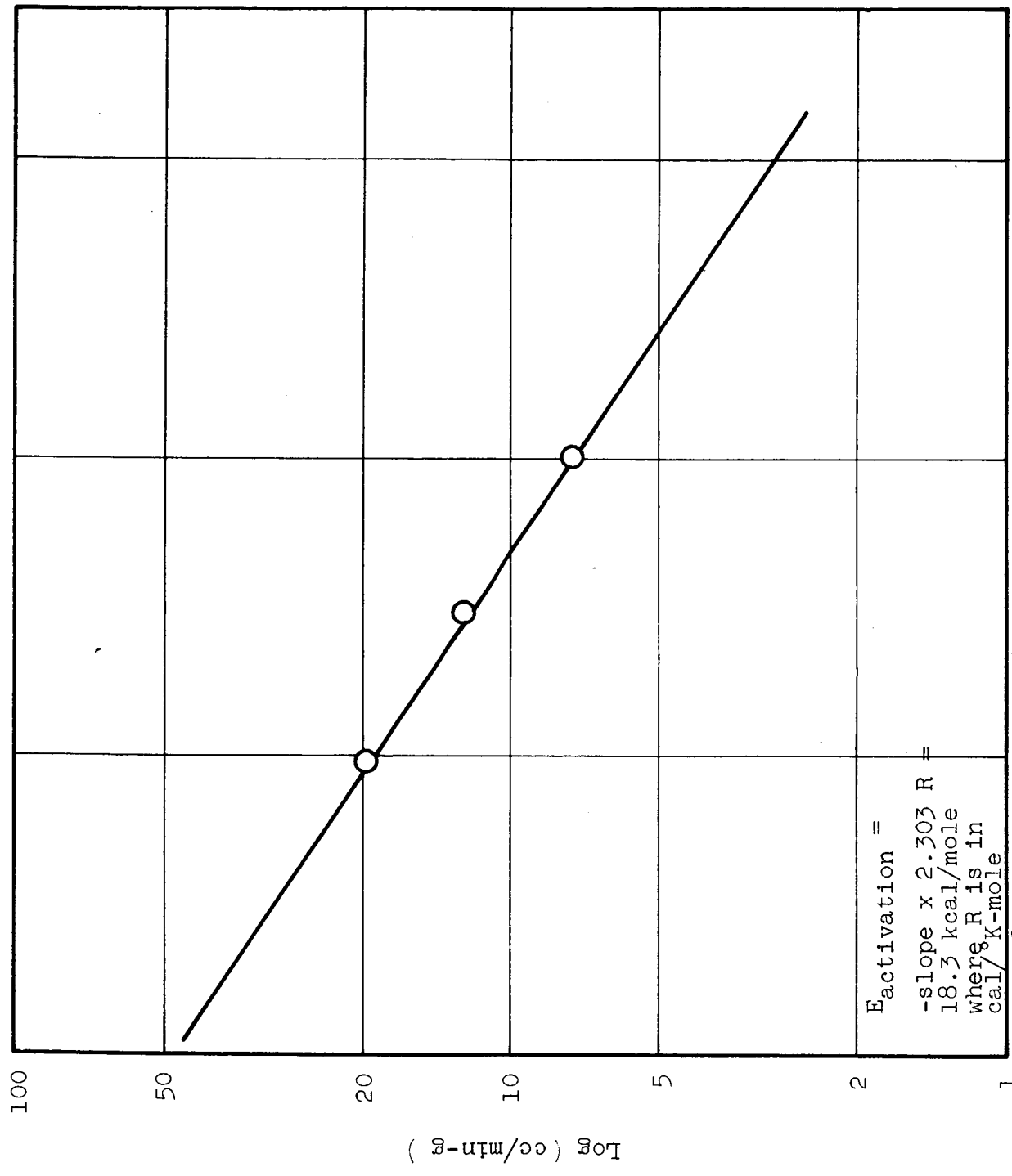

Figure 9. Temperature Dependence Plot for Englehard Rhodium Catalyst Decomposition of Aerozine-50.

(2) Among those tested, Raney nickel and rhodium metals are the best decomposition catalysts for N_2H_4. Reduced stabilized nickel showed some utility.

(3) Cobalt metal catalysts produce NH_3 almost exclusively at very high rates. This agrees with data reported in reference 3.

(4) Activation energies for N_2H_4 decomposition were found to be 18 kcal/mole for a rhodium catalyst with 50/50 mixture of fuels. This agrees with reference 2 and is expected in a heterogeneous catalytic reaction.

(5) UDMH exhibits very little tendency to undergo decomposition at these temperatures and with the catalysts tested.

c. High Temperature Reforming Tests

Table 4 shows gas evolution rates at 200-500°C for blank tests with porcelain chips, and for tests with Girdler G-56B commercial nickel base reforming catalyst.

Assuming that gas evolution with the blank tests was due to nonheterogeneous thermal decomposition of the UDMH, a significant amount of thermal decomposition was found at 500°C. Carbon deposition was noticed on the porcelain chips in the area used to control the catalyst bed temperature.

Table 5 lists the pertinent data found at 500°C using the nickel-base reforming catalyst.

In addition to the data in Table 5, we know that some carbon deposition and NH_3 formation occur if hydrogen and N_2 balances are made on the output gas with respect to the moles of C, CO_2, CO, and CH_4 present in output gas. The amounts of each cannot be determined as yet, because we lack a reliable method. However, we expect to be able to analyze at least UDMH by a KIO_3 oxidation method, without interference from the reaction products (Ref. 4).

d. Conclusions

The reformer system is performing as expected, with regard to equipment and techniques. The results on the G-56-B catalyst fall in between systems 5 and 6 of Table 1; this is reasonably close to expectations.

It seems that the UDMH steam reforming to H_2 will be a feasible operation, but it needs much experimental work with catalysts, flow rates, temperatures, and system pressure for optimum results.

Table 4

GAS PRODUCTION RATES ON BLANK PORCELAIN PREHEATER CHIPS AND WITH NICKEL BASE REFORMING CATALYST

(Pressure 25 psig)

Catalyst	Temperature, °C	Gas Evolution* Liters/hr at 25°C	UDMH Input, mole/hr	H_2O Input, mole/hr
G-56B	293-297	0.252	0.106	0.863
G-56B	395-398	3.22	0.103	0.839
G-56B	498-500	7.23	0.106	0.863
Porcelain Chips	190-197	0	0.104	0.847
Porcelain Chips	293-296	0.038	0.107	0.868
Porcelain Chips	393-396	0.674	0.102	0.831
Porcelain Chips	492-494	4.46	0.104	0.847

Maximum gas volume/hr for UDMH decomposition with 0.105 mole/hr UDMH input = 12.9 liters/hr.

Maximum gas volume for complete reforming to CO_2 with 0.105 mole/hr UDMH input = 23.2 liters/hr.

Catalyst bed, 6 in. long (43 ml volume) with 10-in. porcelain chips preheater, and 4 in. porcelain chips after catalyst.

*Doesn't include NH_3 or CO_2 produced.

Table 5

UDMH REFORMING DATA FOR GIRDLER G-56-B CATALYST,
NICKEL-BASE 1/8-in. TABLETS

Input UDMH - 0.106 mole/hr, or 6.36 g/hr

Input H_2O - 0.863 mole/hr, or 15.20 g/hr

Total input weight - 21.56 g/hr

Gas Analysis (mole-%): H_2, 52.0; N_2, 13.5; CO, 0.6; CH_4, 21.0; CO_2, 12.9; C_2H_6, 0.03.

Total gas output (minus any NH_3 formed) = 8.30 liters/hr at 25°C or 0.337 mole/hr

Average molecular weight of gas output = 14.1

Output as gas = 4.75 g

% Reforming to CO_2 = 20.5%

% Reforming to CO = 0.95%

Moles H_2 per 100 g UDMH input = 2.75

Moles H_2 per 100 g total input = 0.81

$$\text{Hydrogen efficiency} = \frac{\text{moles } H_2 \text{ output}}{\text{moles } H_2 \text{ per UDMH input}} \times 100 = 37.4\%$$

Note: Complete material balance cannot be calculated since no UDMH, NH_3 or water was determined in the product stream.

C. FUTURE WORK

1. Next Quarter

During the next quarter we will concentrate on the medium- to high-temperature decomposition and steam reforming of UDMH. UDMH is the more difficult component to decompose to H_2. When the problem is solved the greater part of the reforming of Aerozine-50 will be solved.

Some continuation of low-temperature N_2H_4 decomposition will be tested to pin down completely the optimum conditions and catalysts for a workable system using Aerozine-50 as the fuel exclusively.

2. Next Month's Work

During the next one to two weeks we will calibrate the VPC with the expected reformer gas components over the expected composition ranges. When this is finished, the analysis of reformer tests will be routine and rapid.

We will then start reforming tests according to the program shown in Table 6.

Table 6

CATALYST TESTING VARIABLES

Catalyst	UDMH Input, g/hr	H_2O Input, g/hr	Temperature, °C	Pressure, psig
G-47 iron oxide	6.3	15.2	350,500,650	50
Girdler catalyst used for NH_3 dissociation	6.3	15.2	350,500,650	150
G-56 nickel base catalyst	6.3	15.2	350,500,650	50
Girdler, used for steam reforming and NH_3 decomposition	6.3	15.2	350,500,650	150
G-43 platinum on alumina	6.3	15.2	350,500,650	50
Girdler catalyst, used for oxide of N_2 reduction	6.3	15.2	350,500,650	150
ICI-35-4	6.3	15.2	350,500,650	50
Girdler catalyst used for NH_3 dissociation	6.3	15.2	350,500,650	150

Other experimental catalysts are to be tested also. The data on these catalysts are given in Table 7.

Table 7

EXPERIMENTAL CATALYSTS TO BE TESTED FOR
UDMH STEAM REFORMING

1.	T-312	Nickel-copper oxides on oxide base	Girdler catalyst
2.	T-313	Low nickel-copper oxide on oxide base	Girdler catalyst
3.	T-315	Low copper oxide on oxide base	Girdler catalyst
4.	T-317	High copper oxide on oxide base	Girdler catalyst
5.	T-366	Copper metal stabilized	Girdler catalyst
6.	T-310	Nickel oxide catalyst on oxide base	Girdler catalyst
7.	T-1144	Nickel oxide	Girdler catalyst
8.	Pyrolyzed acrylonitrile (Monsanto Company) with noble metals		
9.	Molecular sieve with noble metal (Union Carbide Company)		

For details see Appendix II.

III. TASK II DECOMPOSITION OF N_2O_4

A. BACKGROUND

The objective of this task is to decompose nitrogen tetroxide to N_2 and O_2 by thermal and catalytic means to provide an oxygen-rich stream for a fuel cell. The decomposition of N_2O_4 occurs in several steps, depending on the conditions used. It is generally accepted that the decomposition occurs as shown below.

$$N_2O_4 \longrightarrow 2NO_2 \qquad (8)$$

$\Delta H = +13.9$ Kcal/g-mole
complete above 140°C

$$2NO_2 \longrightarrow 2NO + O_2 \qquad (9)$$

$\Delta H = +13.5$ Kcal/g-mole
complete above 600°C

$$2NO \longrightarrow N_2 + O_2 \qquad (10)$$

$\Delta H = -21.5$ Kcal/g-mole
catalytic

Reactions (8) and (9) are homogeneous and thermal in nature and are reversible (Ref. 13). It is evident that any oxygen liberated by reaction (9) must be used or otherwise removed from the reaction site before the temperature is reduced. The oxygen liberated by reaction (10) is not recombined when the temperature is reduced.

If a gas stream of N_2O_4 is fed to a reactor operated at 300-600°C, containing a catalyst for reaction (10) (decomposition of NO) the product stream on cooling would be expected to contain N_2, O_2, NO, and N_2O_4 or NO_2 in varying ratios, depending on the degree of completion to which reaction (10) is carried. Several investigators have found that NO can be decomposed on suitable catalysts when it is contained in high dilution in a stream of inert gas or in a stream containing carbon monoxide. (Ref. 14 and Ref. 15). It is interesting to note that in this work there are indications that reaction products, particularly oxygen, interfere with the decomposition of nitric oxide.

Several studies (Ref. 16, 17) have been made at much higher temperatures (800-1400°C) where nitric oxide (NO) has been decomposed. It is not clear if these results were thermal or catalytic decomposition. In reviewing this work it also becomes apparent that there is some disagreement about the reaction products formed.

The greatest difference between the work now being done and that done by previous workers is in the concentration of nitrogen oxides in the reactor stream. In the earlier work a maximum of 2000 ppm NO_2 or NO in the gas stream was used. In the work reported here pure N_2O_4 is fed to the reactor with no inert gas dilution.

Our approach to finding the best catalysts and operating conditions for decomposing N_2O_4 to nitrogen and oxygen is based on studies utilizing the reactor shown schematically in figure 10 and photograph 11. This reactor system was designed to permit operation from 50-800°C, using a wide range of flow rates. The residence time and space velocity of the reactants can also be varied easily. The analysis of the product stream is determined by cooling the gas stream from the reactor and passing it through a time delay tube of adequate residence time to assure that reaction (11) is complete to NO_2.

$$2NO + O_2 \underset{\text{room temperature}}{\rightleftharpoons} 2NO_2 \qquad (11)$$

The calculation of the tube size was based on the work of Treacy and Daniels (Ref. 18). This calculation was checked using high flow rates of N_2O_4 thermally decomposing to $NO + O_2$ at 600°C and feeding the mixture to the delay tube. A cold trap following the tube collected the N_2O_4 formed. No gas was detected downstream from the trap, indicating all the $NO + O_2$ had recombined.

The NO_2 in the product stream was condensed and frozen out in the cold trap using a Dry Ice/Triclene mixture. The remaining products, NO, N_2, O_2, were passed to a wet test meter for total volume or to either a VPC or oxygen analyzer for composition determination.

The reactor temperature was measured and controlled using iron-constantan thermocouples with a West controller and a Honeywell recorder. The feed flow rates were determined using calibrated flow meters manufactured by Brooks Instruments.

B. RESULTS AND DISCUSSION

Six catalysts have been evaluated for decomposition of N_2O_4 to N_2 and O_2. They are listed in Table 8 and are described in detail in Appendix II.

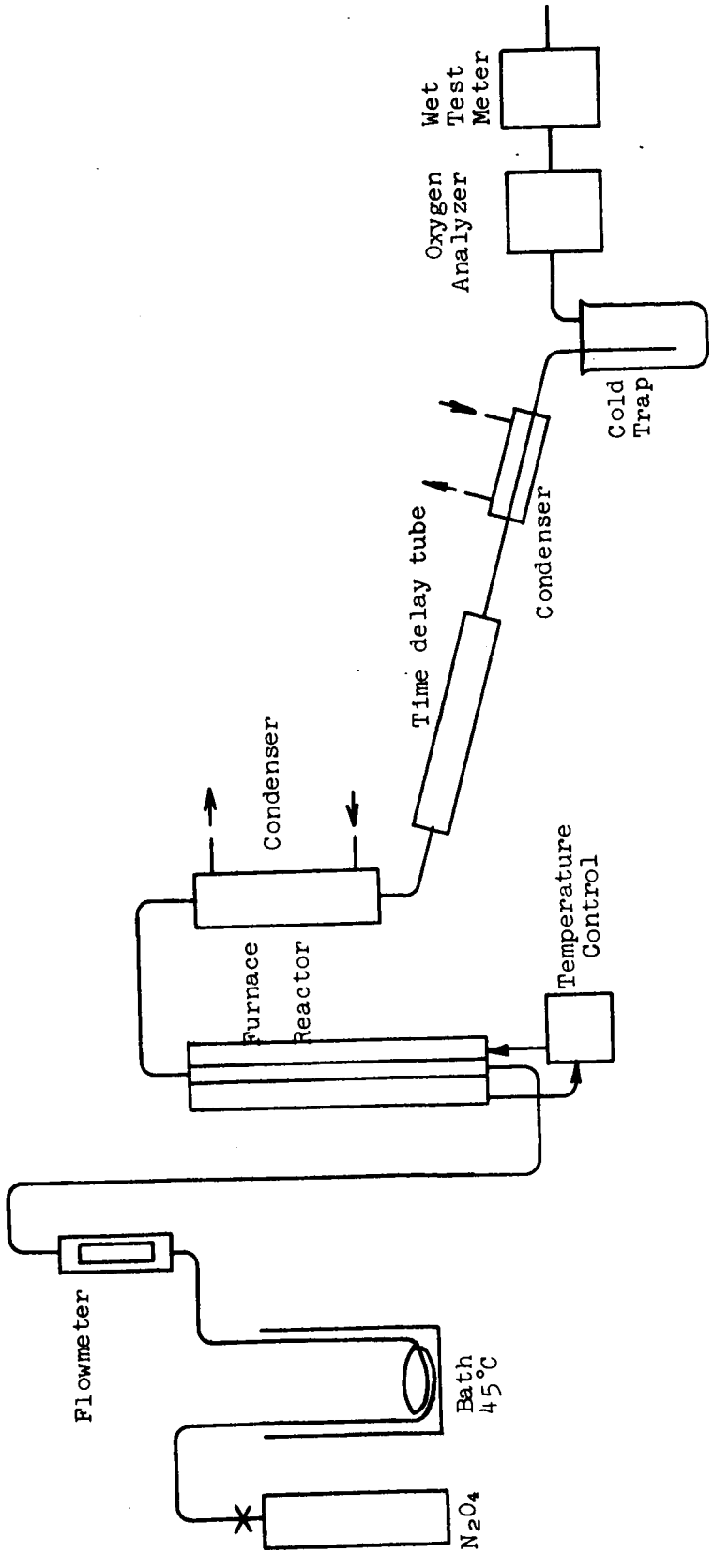

Figure 10. N_2O_4 Reactor Flow Diagram

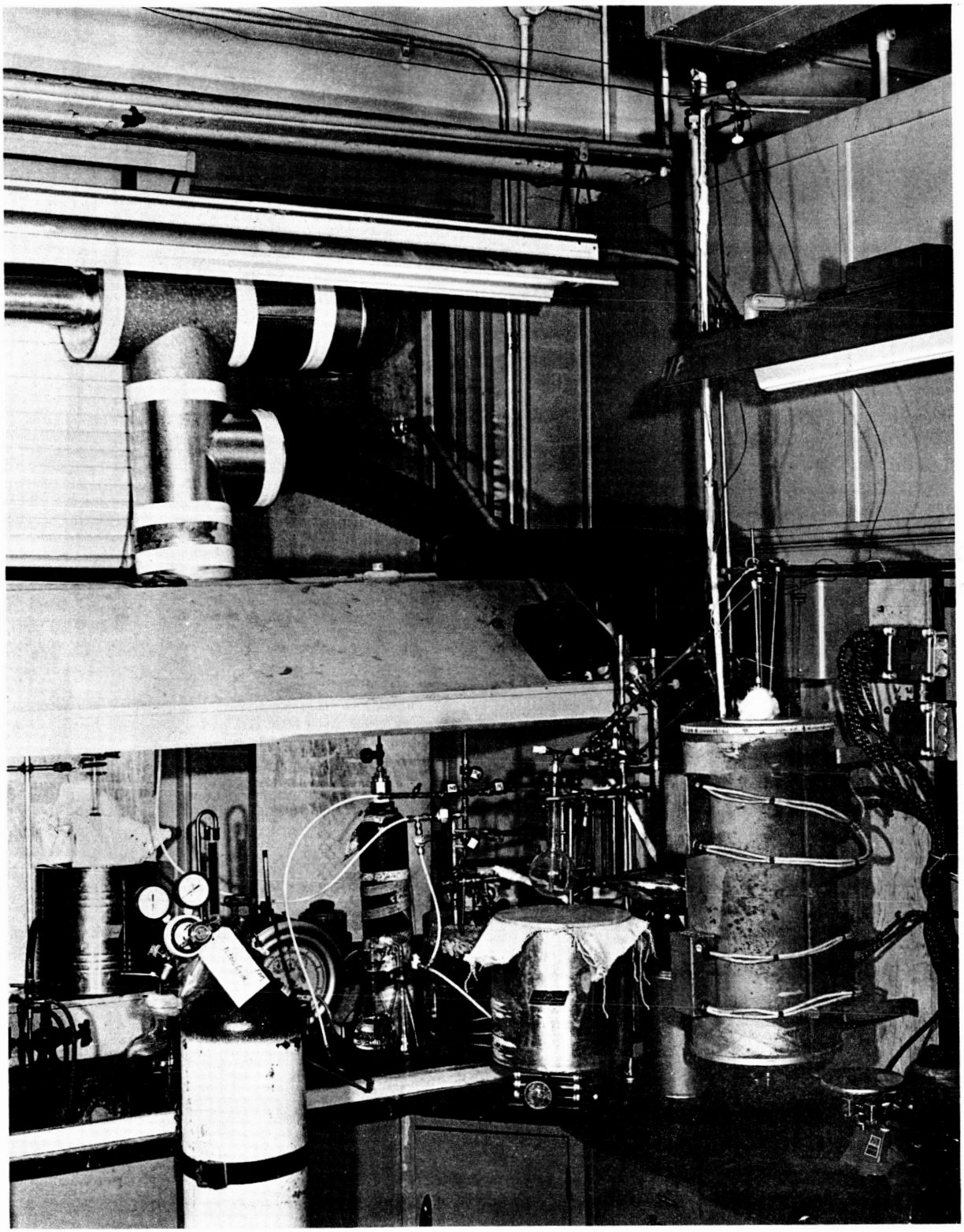

Figure 11. N_2O_4 Reactor Photograph

Table 8

N_2O_4 CATALYSTS

No.	Catalyst	Manufacturer	Temp. Range, °C
1	G-43	Girdler	100-500
2	T-312	Girdler	100-800
3	T-313	Girdler	100-800
4	T-317	Girdler	200-600
5	Hopcalite	MSA	200-400*
6	II-077	Engelhard	200-800

*Contains MnO_2 which decomposes near 500°C

The catalysts were packed in reactor tubes, which are, 22 in. to 26 in. long by 3/4 in. I.D.S.S. The tubes were packed at the lower end using 6-8 in. of number 12 F porcelain beads, which were separated from the catalyst by a fine mesh stainless steel screen. The catalyst bed was 4 in. deep for catalysts 1 through 4, and 12 in. deep for catalysts 5 and 6.

The system was flushed with dry nitrogen, as the reactor was heated to test temperatures. The flush was continued for one hour after each test temperature was reached. The N_2O_4 flow rates are given in test data summary (Table 9). The exhaust gases were passed through the cold trap and then to a wet test meter to measure N_2 and O_2 evolved.

The catalysts tested did not decompose the N_2O_4, as evidenced by the fact that no gas was evolved (Table 9). It will be noted that two flow rates for N_2O_4 were used in the various tests, and that 4 in. and 12 in. catalyst beds were used.

Since the expected decomposition to N_2 and O_2 did not occur, it was felt that tests should be made using nitric oxide feed instead of nitrogen tetroxide to define the apparent lack of activity of the catalysts to promote reaction (10). Duplicate tests were therefore run to determine the activity of the various catalysts for NO decomposition. The nature of these tests is only qualitative at the present time since accurate analysis of the product gases has not been made. This analysis will be made on a newly installed gas chromatograph.

Table 9

N_2O_4 REFORMER DATA

Run Number	Catalyst Number	Reactor Temperature, °C	N_2O_4 Feed Rate, g/hr	Gas Evolved*	Remarks
74601-1	G-43	102	40	0	No decomposition of NO
74601-2	G-43	303	40	0	No decomposition of NO
74602-1	G-43	500	40	0	No decomposition of NO
74605-1	G-43	800	20	0	No decomposition of NO
74603-1	T-312	99	40	0	No decomposition of NO
74603-2	T-312	300	40	0	No decomposition of NO
74603-3	T-312	500	40	0	No decomposition of NO
74604-1	T-312	800	40	0	No decomposition of NO
74606-1	T-313	100	20	0	No decomposition of NO
74606-2	T-313	300	20	0	No decomposition of NO
74606-3	T-313	496	20	0	No decomposition of NO
74606-4	T-313	800	20	0	No decomposition of NO

* Wet test meter

Catalysts 2 through 6 were tested using NO feed at temperatures similar to those used for N_2O_4 tests. The five catalysts tested all showed some degree of activity for NO decomposition, as noted by the appearence of the brown gas NO_2 and the collection of N_2O_4 in the Dry Ice cold trap and some blue solids assumed to be N_2O_3.

Two methods of separating the NO from the product gas stream were tried, neither of which was quantitative. The NO was absorbed in a ferrous sulfate trap and the NO was condensed in a liquid air trap. The ferrous sulfate trap was too limited in its ability to absorb NO in extended runs. The liquid air trap caused volume fluctuations at the wet test meter as the liquid air evaporated or was replenished. (See data in Table 10).

The appearance of crystallized N_2O_4 in the Dry Ice trap during runs using NO feed indicated some catalytic activity for decomposing NO. The complete lack of activity of these catalysts for N_2O_4 decomposition under similar conditions indicated some poisoning of the catalyst by oxygen or deactivation due to the presence of NO_2. The calculated residence times of 10-30 seconds are more than adequate for the reaction. The space velocities for the reactor range from 45-100, which are much lower than the values given by other investigators for the NO decomposition (Ref. 15).

One other major difference between our test conditions and those used by other investigators is the concentration of nitrogen oxides in the gas stream. As can be seen from the references quoted, the successful catalytic decomposition of NO has been carried out in concentration of 2000 ppm or less. It is not immediately apparent why higher concentrations of NO do not give high decomposition rates.

C. FUTURE PLANS

The catalyst evaluations will continue to include those listed in Appendix II and any additional ones that appear to have activity for decomposition of nitrogen tetroxide. A further effort will be made to determine the relationship between nitric oxide decomposition and nitrogen tetroxide decomposition by catalytic means.

To define the extent of nitric oxide decomposition activity of the catalysts and the factors affecting the reaction, two additional feed materials will be tried. The first will be nitric oxide with oxygen added in various multiples or fractions of stoichometric amount contained in N_2O_4. By this method we expect to define the catalyst poisoning effect of oxygen in the stream. The second additive to the feed will be water vapor in various amounts. Water vapor is known to affect greatly many catalytic reactions even when present in only small quantities.

Table 10

REFORMER DATA USING NITRIC OXIDE

Run Number	Catalyst Number	Reactor Temperature, °C	Gas Evolution Rate, ft^3/hr	Length of Run, min.	Remarks
74607-1	T-313	298	10.6×10^{-2}	30	No nitric oxide trap. Total gas volume, N_2, NO, O_2. White and blue crystals in dry ice trap.
74607-2	T-313	300	10.0×10^{-2}	45*	Same as for 74607-1.
74611-2	T-317	200	6.7×10^{-2}	24*	
74611-4	T-317	400	5.5×10^{-2}	31*	
74612-2	T-317	600	5.6×10^{-2}	30*	
74613-2	Hopcalite	201	5.7×10^{-2}	30*	
74613-3	Hopcalite	299	5.7×10^{-2}	30*	
74614-2	Hopcalite	399	5.3×10^{-2}	30*	
74614-4	Hopcalite	299	3.1×10^{-2}	60*	
74615-1	II-077	200	11.4×10^{-2}	30*	
74615-3	II-077	398	11.0×10^{-2}	30*	
74616-2	II-077	600	4.9×10^{-2}	60*	

* Steady state
Note: NO feed rate = 5.2 g/hr or 0.136 ft^3/hr for all runs.

A new gas chromatograph has been installed and is being calibrated to determine oxygen, nitrogen and nitric oxide concentrations. The product stream will be analyzed with this instrument and material balances calculated.

IV. TASK III. ELECTRODE DEVELOPMENT FOR DIRECT REACTANT USE

A. SUBTASK 3.1 CATHODE OPTIMIZATION STUDIES

1. Background

Work on the previous contract (Ref. 1) had produced cathodes operating on gaseous N_2O_4 with high activity and near reversible potentials in contained acid electrolyte-dissolved N_2H_4 fuel cells. However, coulombic efficiencies were low with a single pass of reactant gas (7.7%) and the electrodes tended to "leak" reactants into the contained electrolyte, causing a gradual degradation of anode performance. This was particularly true if the anodes contained carbon. We are sure that electrode design studies will improve the coulombic efficiencies and this work is discussed in a later section. The problem of preventing reactant leakage into the electrolyte can only be solved by controlling the diffusion of N_2O_4 through the electrodes. The problem associated with this procedure is to maintain the good activity and potential characteristics of the electrode at the same time.

2. Factors Affecting Electrode Performance

An experiment was designed to determine the important factors influencing electrode performance. The details and results of this experiment are given in Tables 11, 12, and 13. The design used was a 1/16 replication of a standard 7 factor statistical design (Ref. 19). This type of design is excellent for fast initial screening of many factors with the object of determining the important ones for further study. The actual tests were run in the half-cell setup shown in Figure 12.

Analysis of the data (Table 13) indicates two factors are significant among those tested: the per cent carbon in the carbon-Teflon matrix and the mesh size of the supporting screen. The effect of carbon is not surprising: higher carbon contents should increase the active catalytic area. In following up this lead, the maximum amount of carbon which can be used will be dictated by the strength of the electrode. The use of fluffed carbon filament, which did not reduce performance, will undoubtedly contribute to electrode strength. The effect of screen mesh size is somewhat unexpected, however, it has been noticed qualitatively that the carbon-Teflon matrix impregnates the larger holes in smaller mesh size screening better and this may promote better electrical contact.

Table 11

EXPERIMENTAL DESIGN FOR N_2O_4 CATHODE OPTIMIZATION

(1/16 Replication of 7 Factor Design)

Factor	Description	High Level	Low Level
A	Electrode cure temperature	325°C	300°C
B	Electrode cure time	5 hours	1 hour
C	% Carbon in carbon-Teflon mixture	60%	40%
D	Electrode thickness	double*	single
E	Platinum catalyst	14.5 mg/in.^{2}	none
F	Mesh size of SS screen	60	30
G	% carbon filament in carbon	20	0

Test No.	Electrode	Level of Factors						
		A	B	C	D	E	F	G
1	37-67222	low	low	low	low	low	low	low
2	53-67225	hi	hi	low	low	hi	hi	low
3	56-67229	hi	low	hi	low	hi	low	hi
4	40-67223	low	hi	hi	low	low	hi	hi
5	42-67225	hi	low	low	hi	low	hi	hi
6	59-67230	low	hi	low	hi	hi	low	hi
7	53-67228	low	low	hi	hi	hi	hi	low
8	55-67229	hi	hi	hi	hi	low	low	low

* about 40 mils.

Table 12

RESULTS OF TESTS: N_2O_4 CATHODE OPTIMIZATION, EXPERIMENTAL DESIGN

Test Conditions

"Beaker" Half-Cell test equipment (see Figure 6).

Electrolyte: 5M H_3PO_4
N_2O_4 Pressure: 5.4 in H_2O
N_2O_4 Rate: 400 ml/min STP

Test Electrode	Electrode Potential vs SHE, volts			
	30°C Results		60°C Results	
	50 ma/cm²	100 ma/cm²	50 ma/cm²	100 ma/cm²
1	0.51	0.24	0.76	0.44
2	0.47	0.24	0.52	0.24
3	0.87	0.65	0.93	0.77
4	0.82	0.64	0.85	0.65
5	0.24	0.24	0.24	0.24
6	0.82	0.55	0.90	0.69
7	0.82	0.53	0.88	0.66
8	0.89	0.74	0.93	0.81

Table 13

ANALYSIS OF DATA: N_2O_4 CATHODE OPTIMIZATION

Factor	Description	Relative Effect* 60°C	30°C
A	Cure temperature	-0.04	-0.01
B	Cure time	0.03	0.06
C	% Carbon	0.16	0.16
D	Electrode thickness	0.04	0.04
E	Platinum catalyst	0.03	0.03
F	Screen mesh size	-0.12	-0.12
G	% Carbon filament in carbon	0.03	0.03

* Relative effect in volts per unit increase in level of parameter on cathode potential at 100 ma/cm^2.

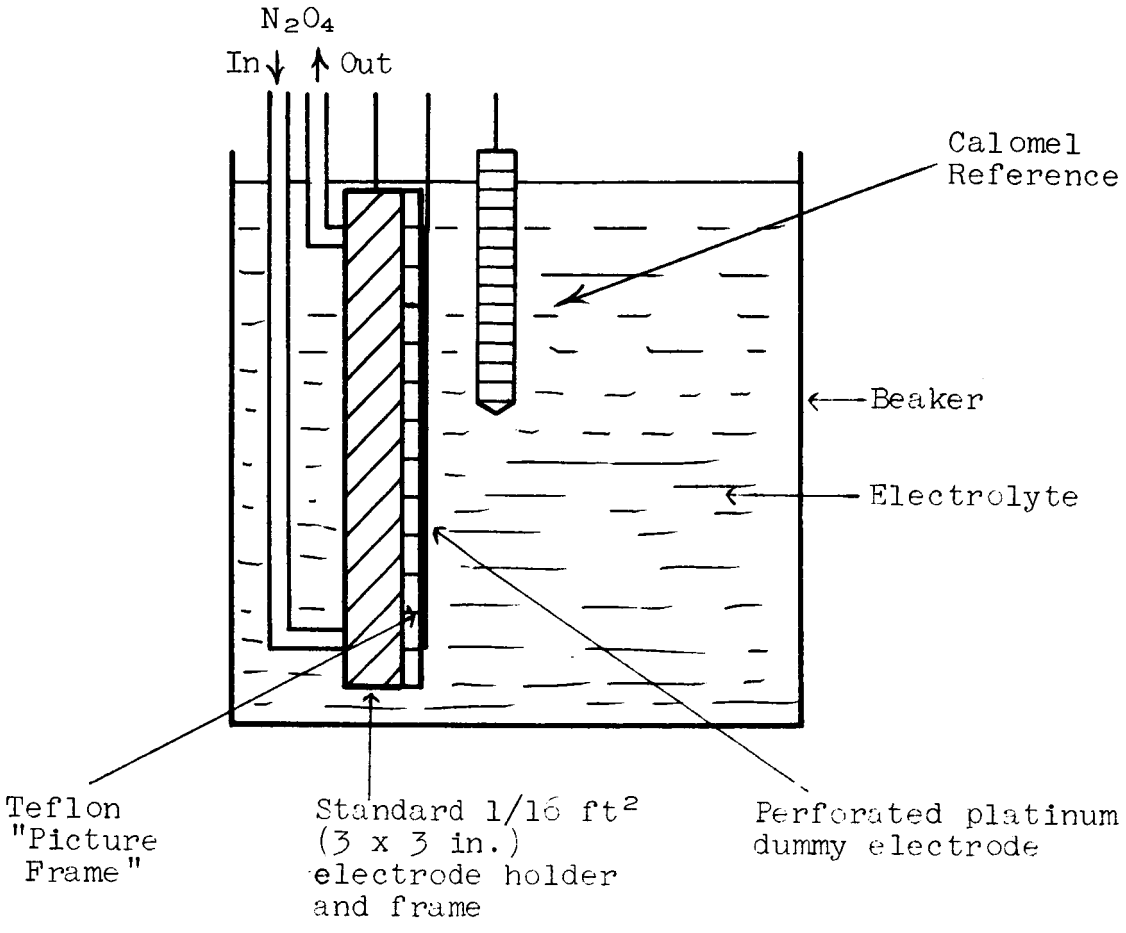

Figure 12. 3 x 3 in. Half Cell

The results of the tests on electrode thickness are significant in that there is a strong indication of lack of diffusion control in the range of thickness investigated here. It is evident that the electrode is essentially saturated with an excess of reactant, and doubling the thickness has not reduced the diffusion rate sufficiently to affect performance at 100 ma/cm^2. This result prompted an investigation of the diffusion characteristics of the electrode (reported in a later section).

Much difficulty was experienced with the half-cell setup used in this investigation, particularly with respect to temperature gradients, excessive decomposition of the electrolyte by the dummy electrode and the high currents required from the power supply. For these reasons it was decided to conduct future tests with standard hydrogen or oxygen counter electrodes in full cells. A screening program in a 5.0 cm^2 glass half cell was initiated to test modifications of MRD carbon/platinum electrodes for this service (presented in Table 14). The major problem was to prevent break-through of the gas, and various diffusion barriers were tested. The best choice for both H_2 and O_2 electrodes was a standard MRD carbon/platinum electrode with the carbon (gas) side sprayed with a Teflon emulsion.

A "full cell" using the best cathode from the experimental design (Electrode 55-67229) and a Teflon-sprayed anode operating on H_2 gas were constructed using the 3 in. x 3 in. electrode holders developed under the previous contract (Ref. 1). The Teflon gasket-spacer was slotted for electrolyte passage. A pumped electrolyte cell test stand was constructed, as shown in Figure 13. Using this equipment, the cathode was characterized and the results are given in Table 15 and Figure 14. In Table 15 the effects of temperature and N_2O_4 flow rate are summarized. The electrode is highly active at room temperature and performance is not substantially improved at the higher temperatures. It should be noted that the lowest N_2O_4 flow rate reported here would represent 8.5% coulombic efficiency at 100 ma/cm^2 for a cell of this size (3 x 3 in.). The improvement of the coulombic efficiency is a major task on this project and is covered in a latter section. (Subtask 3.3 "Design of 1/3 ft^2 Electrodes").

In Figure 5 the full cell data for the H_2/N_2O_4 cell used to test this cathode are plotted for the 60°C run. A comparison of these data with the tests on N_2H_4/N_2O_4 cells made under the previous contract (Ref. 1) indicates the cathode tested here performs somewhat better even at substantially lower N_2O_4 flow rates. The H_2 anode in this work tends to polarize more than the N_2H_4 flow-through anodes used in previous work, but it starts out approximately 0.20 v better. The potential of these two electrodes are nearly identical at 100 ma/cm^2. Since the H_2 electrode is used simply as a counter electrode, we feel this performance is adequate for this work.

Table 14

HYDROGEN AND OXYGEN HALF CELL TESTS

1. 5.0 cm^2 glass half cell with platinum dummy electrode driven by Kordesch-Marko bridge.
2. Electrolyte: 5M H_3PO_4 for H_2 tests, 5M H_2SO_4 for O_2 tests.
3. Temperature: 50-55°C
4. All electrodes: MRD-A platinum/carbon, 4.2 mg Pt/cm^2, carbon layer is 0.015 in. as rolled out for single thickness, 0.030 in. as rolled out for double thickness.

		H_2 Anode Tests			O_2 Cathode Tests		
		Potential vs SHE ma/cm^2			Potential vs SHE ma/cm^2		
Electrode	Description	100	200	Gas Breakthru	100	200	Gas Breakthru
62399-1	1 single carbon thickness	0.04	0.04	slight	0.61	0.47	none
62399-2	2 single carbon thicknesses	0.04	0.04	slight	-	-	-
62399-3	3 single carbon thicknesses	0.04	0.04	moderate	0.79	0.76	none
62399-4	1 double carbon thickness	0.03	0.03	moderate	0.72	0.68	none
62399-5	2 double carbon thicknesses	0.03	0.03	-	0.79	0.76	none
72403-6	1 single carbon thickness with screen on both sides	0.02	0.03	slight	0.75	0.74	none
72403-7	2 single carbon thicknesses with screen on both sides	0.04	0.04	slight to moderate			
72403-8	1 single carbon with sprayed Teflon backing diffusion barrier	0.02	0.03	none to slight	0.84	-	none
72407-9	2 electrodes as 62399-5 above with sprayed Teflon between	0.05	0.05	slight			
72410	Electrode 62399-3 with Metricel VM-6 porous vinyl membrane backing	0.05	0.06	slight			

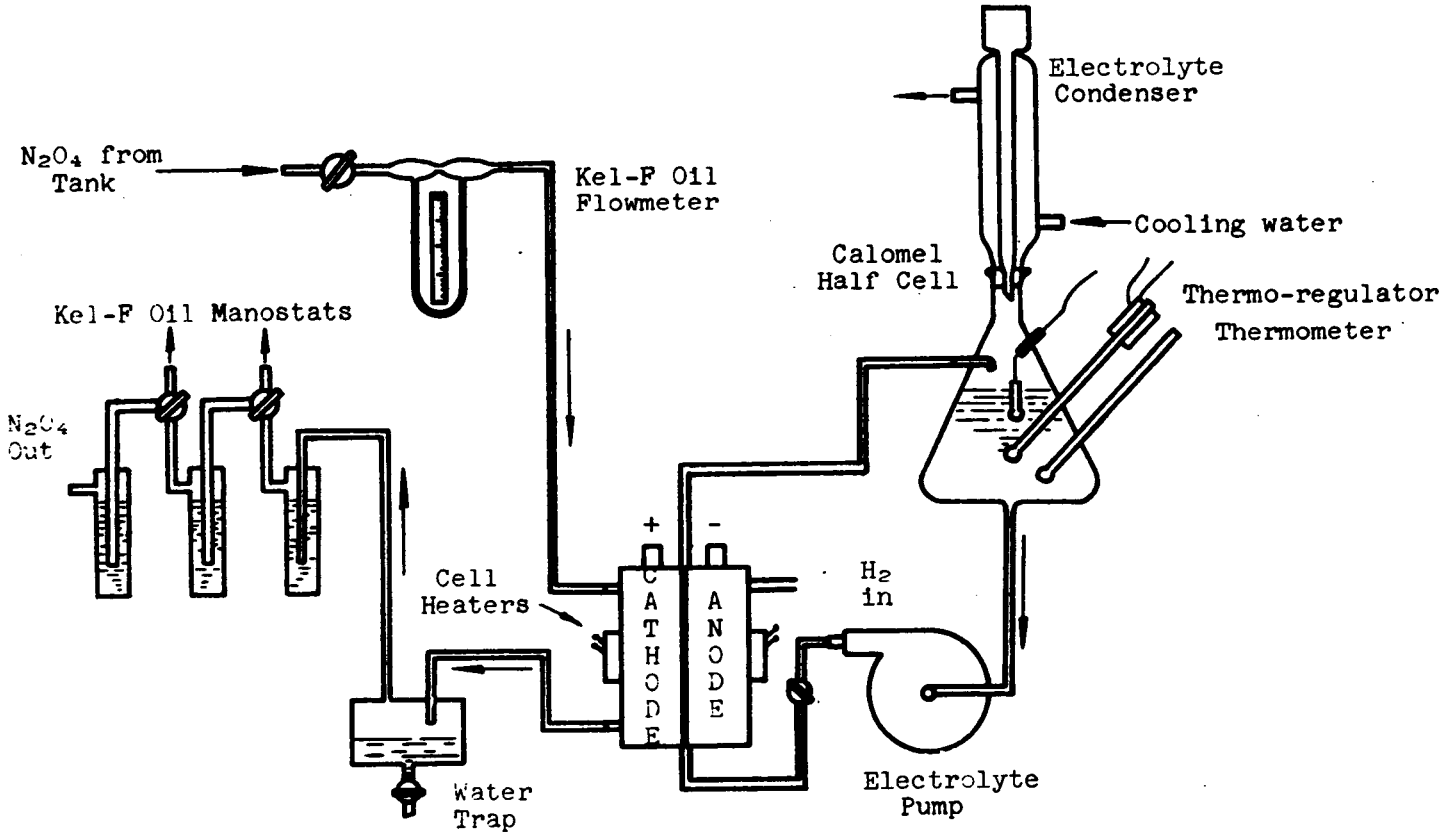

NOTES:
1. All tubing is Teflon or glass. All connections are Teflon or stainless steel Swage-Loks fittings.
2. Electrolyte pump speed controlled by variac.
3. Heating tapes and insulation around electrolyte flask. Tapes and cell heaters controlled by thermo-regulator. Glass wool insulation around cell.
4. N_2O_4 is tank grade. Tank maintained at 40°C in water bath.
5. H_2 is tank grade.

Figure 13. Pumped Electrolyte Cell Test Stand

Table 15

CHARACTERIZATION OF CATHODE 55-67229

Cell No: 72424 (H_2/N_2O_4) Anode: 72428-2 (MRDA Carbon/Pt with Sprayed Teflon Backing)

Electrolyte: 5M H_2PO_4, Pumped "Cell and Test Stand (See ref. 7)" H_2 Fuel: 0 psig, Slight Purge

N_2O_4: 5.4 in H_2O Pressure

N_2O_4 Flow Rate g/min	Current Density ma/cm^2	30°C Tests Cathode Potential vs SHE, volts	60°C Tests Cathode Potential vs SHE, volts	90°C Tests Cathode Potential vs SHE, volts
0.7	0	0.98	1.01	1.11
	50	0.98	1.01	1.04
	100	0.97	1.01	0.97
	150	0.92	1.00	0.96
	200	--	--	0.91
1.2	0	1.02	1.02	1.04
	50	1.02	1.01	1.04
	100	1.01	0.93	0.99
	150	1.00	0.79	0.89
	200	--	--	--
1.6	0	1.02	1.07	1.06
	50	--	1.00	1.06
	100	1.02	0.89	1.00
	150	--	--	1.00
	200	0.90	--	0.89

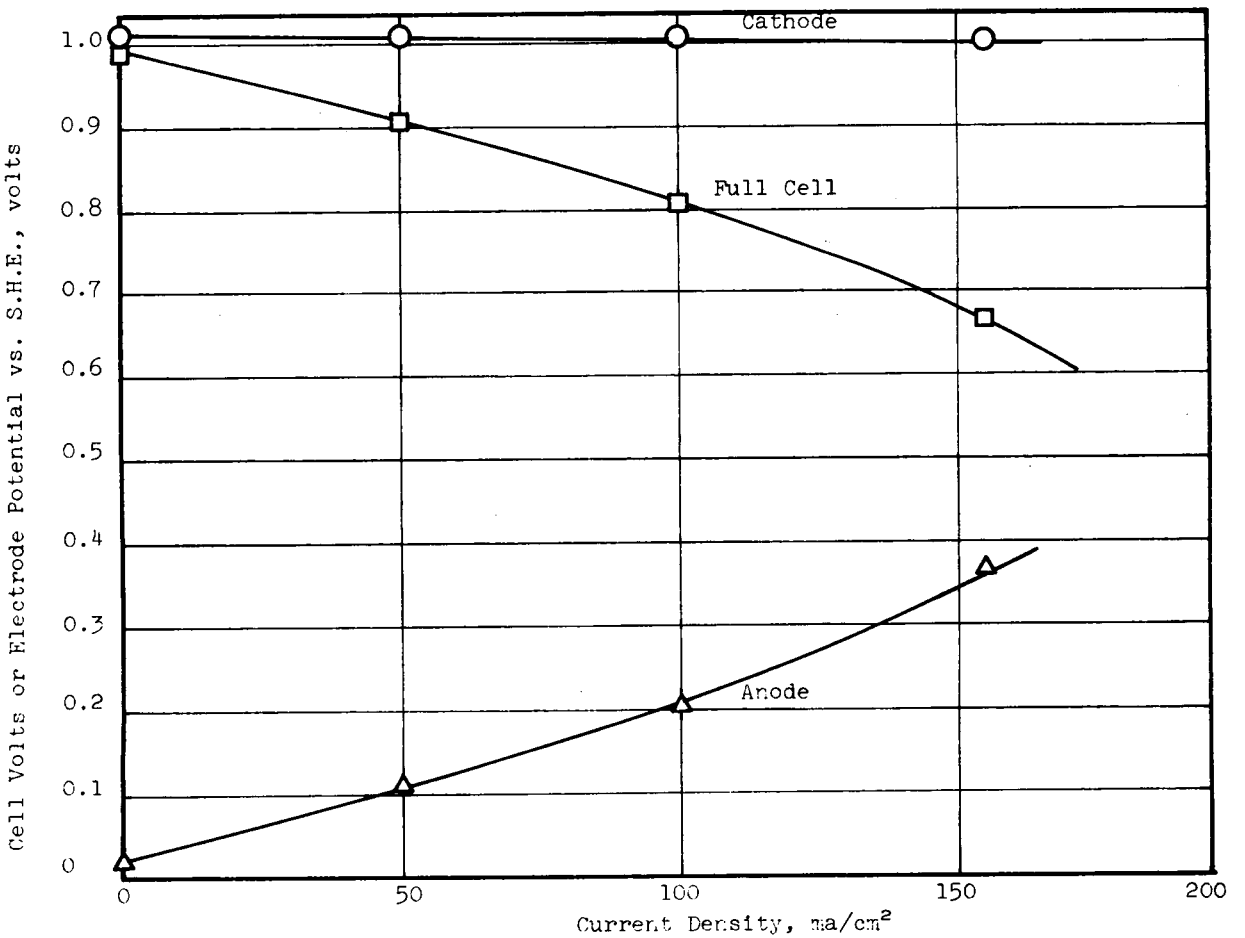

Cathode:	55-67229 (MRC-C double carbon)
Anode:	72423-2 (MRD-A carbon/Pt with sprayed Teflon backing)
Electrolyte:	5M H_3PO_4, pumped
H_2:	0 psig, slight purge
N_2O_4:	5.4 in H_2O pressure, 0.7 g/min flow rate
Temperature:	60°C

Figure 14. Polarization Curve for Cell 72424 (H_2/N_2O_4)

3. Diffusion of N_2O_4 Through MRD-C Cathodes

a. Background

At the temperatures of interest in this work, the N_2O_4 oxidant is actually a mixture of NO_2 and N_2O_4 gases. Both components are soluble in the phosphoric acid electrolyte according to the following equations (Ref. 20):

$$N_2O_4 + H_2O = HNO_2 + HNO_3 \quad (12)$$

$$2NO_2 + H_2O = HNO_2 + HNO_3 \quad (13)$$

In work with wetted-wall columns several investigators have found the absorption rate in water or dilute nitric acid to be directly proportional to the concentration of gaseous N_2O_4 at a fixed temperature (Ref. 21, 22, 23). However, at constant temperature the ratio of NO_2 to N_2O_4 is fixed by the equilibrium constant for:

$$2NO_2 \rightleftharpoons N_2O_4 \quad (14)$$

which is in instantaneous equilibrium. Thus reaction (12) and (13) are equivalent and the oxidant will be considered to be N_2O_4 alone in the following discussion. Peters and Holman (Ref. 20.) showed that both gas-phase and liquid-phase reactions occur in the absorption of gaseous N_2O_4 by aqueous solutions in wetted-wall columns. The major part of the reactions occur in relatively thin gas and liquid films at the boundary between the two phases. The gas-phase reaction was shown to be exothermic, which is consistent with a postulated reaction with water vapor and N_2O_4.

The absorption rates were substantially higher than predicted by the rate equation for a completely gas-phase reaction, indicating a competing liquid-phase reaction in which the reactive ions catalyze the absorption.

The effect of reactions (12) and (13) in our work is clear; any N_2O_4 that diffuses through the electrode and is not consumed electrochemically can dissolve in the electrolyte. In a pumped electrolyte cell, in which "fresh" electrolyte is continually brought to the electrode surface, the amount dissolved in a given time will be determined by the diffusion rate through the electrode and the current drawn from the cell. The effects are a loss of coulombic efficiency at the cathode, and a gradual poisoning of the anode as the HNO_3-HNO_2 concentration builds up in the electrolyte.

The most direct approach to this problem is to limit the diffusion of the N_2O_4 through the electrode to that amount required for the electrochemical reaction at a given current density. It is obvious that operation of a cell below the set current density (and in the limit on open circuit) will leave an excess of N_2O_4 available to dissolve in the electrolyte. Thus, in missions where variable power demand is likely and high electrode efficiencies are desired, the N_2O_4 supply must be controlled by proper instrumentation monitoring the current load on the module. In any case, a primary requirement is for reliable control over the N_2O_4 diffusion through the electrode.

The program developed to work on this problem is:

(1) Develop an analytical technique to measure the amount of N_2O_4 diffusing through the electrode and dissolving in the electrolyte.

(2) Determine the electrode parameters (thickness, formulation, pressing, etc.) controlling the diffusion rate.

(3) Determine the effect of external parameters (N_2O_4 pressure and flow rate, temperature) on the diffusion rate.

(4) Using the above data, design an electrode in which the diffusion rate can be controlled to give minimum N_2O_4 contamination of the electrolyte while, at the same time, supplying enough reactant to support the maximum drain expected from the electrode.

b. Experimental Work

The diffusion cell shown in Figure 15 was constructed. The electrode is clamped between rubber O-rings in the glass cell, N_2O_4 gas is slowly purged on one side and a measured amount of 2M H_2SO_4 electrolyte is exposed to the N_2O_4 diffusing through the electrode on the other side. The amount of N_2O_4 diffusing through and dissolving is determined by analyzing the electrolyte for nitrite ion. This was done by incorporating a known amount of $KMnO_4$ in the 2M H_2SO_4 and titrating the electrolyte sample with standard sodium oxalate solution to determine the amount of $KMnO_4$ consumed in oxidizing the nitrite ion. The reactions involved are:

$$N_2O_4 + H_2O = HNO_2 + HNO_3 \quad \text{(diffusion and solution in the electrolyte)} \quad (15)$$

$$HNO_2 = H^+ + NO_2^- \quad (16)$$

$$5NO_2^- + 2MnO_4^- + 6H^+ = 5NO_3^- + 2Mn^{++} + 3H_2O \quad (17)$$

(oxidation in the electrolyte)

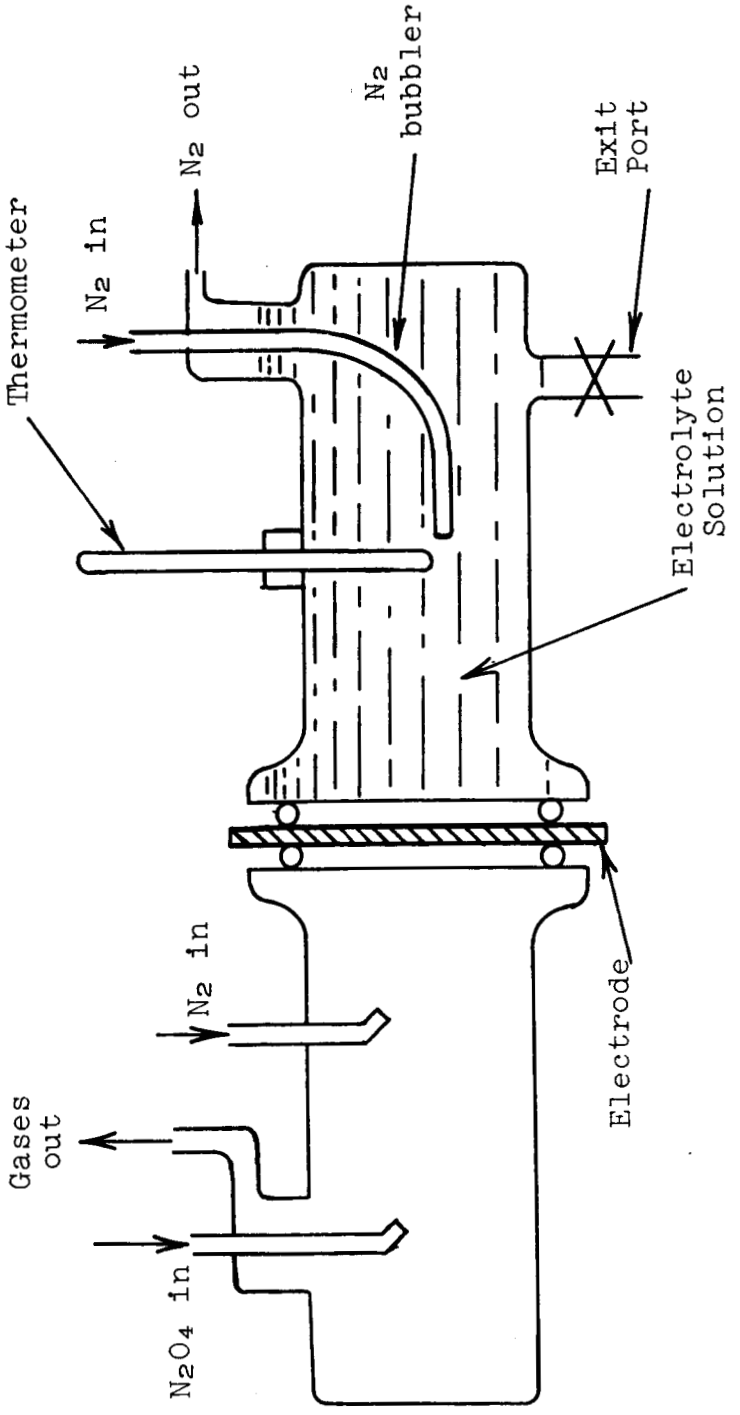

Figure 15. N_2O_4 Diffusion Cell

$$5C_2O_4^{=} + \underline{2}MnO_4^{-} + \underline{16}H^{+} = 10CO_2 + \underline{2}Mn^{++} + \underline{8}H_2O \quad (18)$$

(back titration with oxalate)

The titration of permanganate with oxalate in the presence of nitric acid is a standard method (Ref. 24). However, it is a more complicated reaction in H_3PO_4 solutions because of precipitation of the insoluble Mn II phosphate. Initial work indicated that the titration was reproducible when sufficient time was allowed for precipitation and when slightly oxidizing conditions existed at the end point (to reoxidize any MnIII formed). However, when actual runs were made in the diffusion cell with 5M H_3PO_4 electrolyte, an N_2O_4 diffusion rate which declined with time of exposure was found. This effect was assigned to the precipitation of the manganese phosphate in the pores of the electrodes, reducing the void volume and lowering the rate. In fact the effect was marked enough to justify investigating it as a method of diffusion control in these electrodes. Work in this area is scheduled. Reproducible and accurate measurement by this method, however, dictated the use of H_2SO_4 rather than H_3PO_4 as the electrolyte.

The N_2O_4 diffusion rate through the best electrode from the experimental design (previous section, electrode No. 55-67229) has been determined at three different exposure times and two N_2O_4 pressures at 25°C. The results are tabulated in Table 16. Three conclusions can be drawn from this initial work:

(1) The diffusion rates are substantially higher than the stoichiometric requirement at reasonable current densities - ranging from 2 to 6 times the amount required for operation at 100 ma/cm^2.

(2) The rate is higher at higher N_2O_4 pressures, qualitatively corroborating the results on wetted-wall columns, discussed previously.

(3) The average effect of exposure time is fairly constant indicating that the method is reproducible. The individual values for the 0.5-min. run show substantial variation, probably due to nonattainment of equilibrium conditions and/or the relatively higher percentage error involved in measuring small quantities. Future runs will be made with times of 1 minute of greater.

This work has clearly shown that the N_2O_4 cathode is not diffusion-limited, and at reasonable current densities excess N_2O_4 will be available to dissolve in the electrolyte. Future work will involve determining the effects of external (temperature, pressure, flow rates) and electrode (thickness, formulation, treatments) parameters to acquire control of the diffusion characteristics.

Table 16

N_2O_4 DIFFUSION RATE - ELECTRODE 55-67229

Electrolyte: 2M H_2SO_4 (0.2N in $KMnO_4$)
Temperature: 25°C
N_2O_4 Flow Rate through Cell: 1.6-2.0 g/min.

N_2O_4 Pressure, in. H_2O	Diffusion Rates in g N_2O_4/hr/cm^2 Exposure Times, min. 0.5	1.0	2.0
0	0.34	0.19	0.18
5.4	0.28	0.46	0.55

Mean Values:

0 in. H_2O pressure: 0.24 g N_2O_4/hr/cm^2

5.4 in. H_2O pressure: 0.43 g N_2O_4/hr/cm^2

0.5 min exposure: 0.31 g N_2O_4/hr/cm^2

1.0 min exposure: 0.33 g N_2O_4/hr/cm^2

2.0 min exposure: 0.36 g N_2O_4/hr/cm^2

Stoichiometric Requirement for 100 ma/cm^2:

0.089 g N_2O_4/hr/cm^2

B. SUBTASK 3.2 DEVELOP AEROZINE-50 ANODE

1. Background

In our earlier work (Ref. 1), flow through MRD-A Pt anodes were shown to have high activity on N_2H_4 dissolved in 5M H_3PO_4 electrolyte. Coulombic efficiencies were reduced in this configuration by the spontaneous decomposition of the N_2H_4 and the subsequent loss of H_2. The current contract requires operation on Aerozine-50, a 50-50 by weight mixture of N_2H_4 and unsymetrical dimethyl hydrazine (UDMH), with the fuel not dissolved in the electrolyte but fed to the cell in a pure form.

The major problems in this work will be: (1) to prevent excessive decomposition of the hydrazine by limiting its contact with the electrode (diffusion barriers), and (2) to electro-oxidize the dimethylhydrazine efficiently. The first problem is one of electrode design, while the second problem is more fundamental. The electrochemical oxidation of unsymmetrical dimethylhydrazine at reasonable efficiency and potentials is considered the most difficult problem in this task. Initial work on a preceding contract indicated the methylhydrazines were relatively poor electrochemical fuels (Ref. 25). King and Bard investigated the electro-oxidation of the methylhydrazines on Pt electrodes in H_2SO_4 solutions (Ref. 26). They found the oxidation of UDMH was a complex reaction. Chronopotentiometric measurements indicated an initial 2-electron reaction starting, with their electrodes and conditions, at about +0.8v vs. S.H.E., and which did not generate N_2 as a product. Further investigation indicated that during the initial stage a product is formed which is not oxidizable but which decomposes by a first-order reaction (half-life of 25 min.) to form N_2 and another product, oxidizable by a further 2-electron process. Controlled potential coulometry indicated an overall electron change that varied with conditions (n values of 4.7 to 5.9). Product analysis showed N_2, CH_3OH, HCHO, $(CH_3)_2NH$, and an unidentified soluble, yellow-colored species.

The mechanism proposed to account for these facts is an initial oxidation to 1,1-dimethyldiazene:

$$(CH_3)_2N\text{-}NH_3^+ \longrightarrow (CH_3)_2N^+\text{=}NH + 2H^+ + 2e^- \qquad (19)$$

After this initial stage there are several reaction paths. One would be a rearrangement to the hydrazone, hydrolysis of the hydrazone and subsequent oxidation of the methylhydrazine formed:

$$(CH_3)_2N^+\text{=}NH \longrightarrow CH_2\text{=}NH\text{-}NH\text{-}CH_3 + H^+ \qquad (20)$$

$$CH_2\text{=}NH\text{-}NH\text{-}CH_3 + H_2O \longrightarrow CH_3NH\text{-}NH_2 + HCHO \qquad (21)$$

$$CH_3NH\text{-}NH_2 + H_2O \longrightarrow CH_3OH + N_2 + 4H^+ + 4e \qquad (22)$$

This path accounts for the 6e overall change and the formation of CH_3OH, HCHO, and N_2.

An alternate and competing path which would account for the yellow product and for $(CH_3)_2NH$ would involve hydrolysis of the diazene, followed by oxidation to N-nitrosodimethylamine (yellow).

$$(CH_3)_2N^+=NH + H_2O \longrightarrow (CH_3)_2N\text{-}NHOH + H^+ \quad (23)$$

$$(CH_3)_2N\text{-}NHOH \longrightarrow (CH_3)_2N\text{-}N=O + 2H^+ + 2e \quad (24)$$

$$(CH_3)_2N\text{-}N=O + H_2O \longrightarrow (CH_3)_2NH + HNO_2 \quad (25)$$

The approach we have taken has been to screen electrode catalysts with the hope that one would be found that:

Promotes reaction (19) at reasonable activity and potentials;

Promotes reaction (20) and/or (23) and subsequently (22) and (24) so that greater coulombic capacity can be realized from the UDMH portion of the fuel;

At a minimum, promotes the electro-oxidation of N_2H_4 in the presence of UDMH without being "poisoned" by the UDMH or any of its many oxidation products.

2. Results and Discussion

A catalyst evaluation program was started using UDMH or Aerozine-50 as the fuels, H_3PO_4 electrolyte, and MRD-A electrodes made with noble metal catalysts. The activities of each electrode were determined in a glass half cell with a Pt dummy electrode in the electrolyte and the fuel used in the undiluted state on the reverse side of the electrode. The results of this work are summarized in Table 17. The electrode catalysts were:

Electrode No.	Description
70434-10A	Pt on Pt screen
70453-4	90-10, Pt and Pd on Pt screen
70434-3B	90-10, Pt and Ru on Pt screen
70459-60	Proprietary Monsanto CH_3OH electrode

None of these electrodes demonstrated high activity on UDMH alone. The effect of the hydrazine component in the Aerozine-50 is shown in the tests on Electrode 70453-4. Longer term tests were run on Electrode 70453-4 with Aerozine-50 to determine if progressive poisoning or loss of activity occurred. The results, shown in Table 18, are encouraging.

Table 17

AEROZINE-50 AND UDMH ELECTRODE TESTS

IR Free Electrode Potentials vs SHE, volts

Temp., °C	Current Density ma/cm²	Electrode No* 70434-10A	Electrode No* 70453-4	Electrode No† 70453-4	Electrode No† 70434-3B	Electrode No† 70459-60
30	0	-0.23	-0.26	+0.46	+0.10	+0.15
	50	+0.04	---		+0.17	---
	100	+0.09	+0.16	No	+0.36	+0.38
	150	+0.16	+0.25		+0.42	+0.40
	200	+0.23	+0.29	Activity	+0.47	+0.41
	250	---	+0.31		---	+0.42
60	0	-0.05	-0.01	+0.30	+0.09	+0.07
	50	-0.16	---	+0.55	+0.38	+0.18
	100	-0.15	+0.02	---	+0.40	+0.22
	150	+0.15	+0.05	---	+0.56	+0.24
	200	+0.21	+0.13	---	---	+0.26
	250	---	+0.18	---	---	+0.28
90	0	-0.11	+0.02	+0.18	+0.09	+0.12
	50	-0.17	+0.01	+0.41	+0.27	+0.16
	100	-0.17	+0.02	+0.43	+0.35	+0.24
	150	+0.06	+0.03	+0.58	+0.59	+0.30
	200	+0.07	+0.04	---	---	+0.32
	250	---	+0.06	---	---	+0.37

*Fuel: Aerozine 50
†Fuel: UDMH alone

Table 18

TWO HOUR TESTING OF ELECTRODE 70453-4

Current Density: 100 ma/cm²
Fuel: Aerozine-50

Temperature, °C	IR Free Potential vs SHE, volts	
	Initial	After 2 Hours
30	+0.02	+0.13
60	+0.05	0.0
90	+0.02	+0.02

Several experimental difficulties were encountered with this technique. First, it was qualitatively observed that diffusion rates of the fuel through the electrodes varied greatly, raising the possibility that the diffusion rate rather than the catalyst was determining electrode performance. Second, gas-bubble formation on the electrode surface masked off active areas and caused erratic performance. The screening cell was redesigned to use dissolved fuel, with a stream of fuel-electrolyte solution pumped across the electrode surface to sweep away gas bubbles. This had the additional effect of reducing concentration polarization in the cell. With these modifications the true activity of the catalysts could be determined. A representation of the cell is shown in Figure 16. A Kordesch-Marko bridge was used to obtain IR-free potentials.

The electrodes listed in Table 19 were evaluated in this cell and the results are given in Table 20. None of the catalysts tested showed high activity on UDMH fuel at reasonable potentials. The best UDMH catalyst was Rh black (Engelhard Industries) which operated at +0.56v to SHE at 100 ma/cm², 60°C, and formed a yellow product. Tests with this electrode on Aerozine-50 fuel indicated only the N_2H_4 potential with no yellow color in the electrolyte, even after 1 hr at 100 ma/cm². These results suggest that UDMH is relatively inactive in the presence of N_2H_4 and will act as an inert diluent at least for times up to 1 hr with the catalysts tested. The coulombic efficiency per lb of fuel will be correspondingly reduced; thus further effort in this area is worthwhile. At a minimum, however, it appears that a catalyst (Rh) has been found which will utilize the N_2H_4 portion of Aerozine-50 with good activity without interference from the UDMH portion, at least on short-range testing.

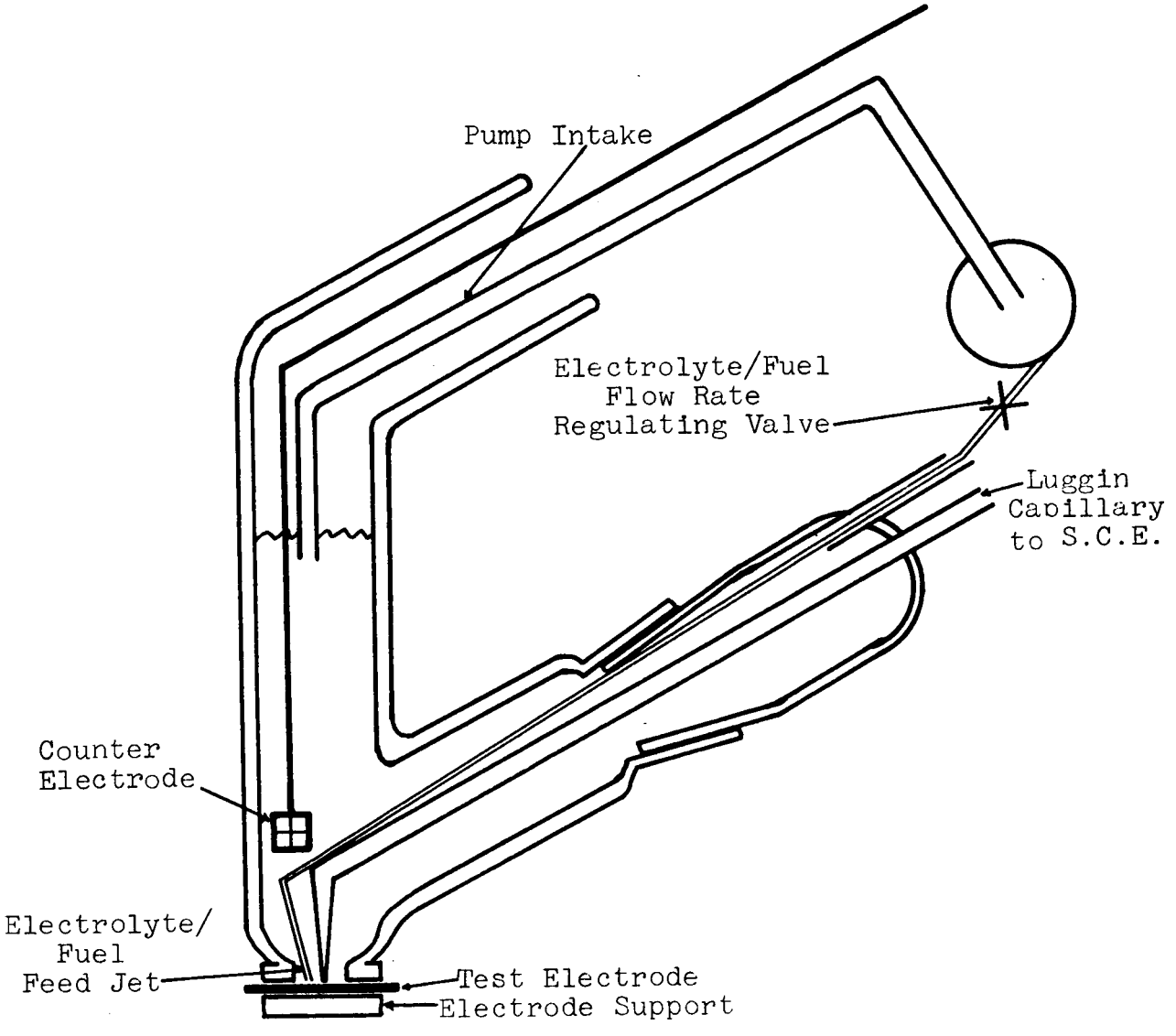

Figure 16. Fuel Catalyst Screening Cell

Table 19

UDMH ELECTRODE DESCRIPTION

Electrode Number	Description
70434-10A	Pt on Pt screen (lab made Pt)
79-67240	Pt on s.s.screen (Engelhard Pt)
56838	MRC chelate catalyst on carbon substrate
50-67226	Rh on Pt screen (Engelhard Rh)
70459-60	MRC quaternary noble metal alloy catalyst on Pt screen
70457-8	MRC ternary noble metal alloy catalyst on Pt screen
70485-6	Pt-Ru (90-10) alloy on Pt screen
68729-3	Raney Ni on carbon on s.s.screen
73233-2a	Ni_2B on Pt screen
73233-1a	Co_2B on Pt screen
71202-7	Mo powder (200 mesh) on s.s.screen
71210-1	Mo powder (200 mesh) +4% (Engelhard Pt) on s.s.screen
75358	Pt-Ru (70-30) alloy on Pt screen

Table 20

UDMH ELECTRODE TEST RESULTS

Temperature: 60°C
Electrolyte: 5M H_3PO_4
Fuel: 3M in all cases

Electrode	Fuel	Electrode Potential (volts) vs SHE at Indicated Current Density				
		0 ma/cm²	50 ma/cm²	100 ma/cm²	150 ma/cm²	200 ma/cm²
70434-10A	N_2H_4	0.26	0.35	0.36	0.38	0.40
70434-10A	UDMH	0.36	0.76	0.78	-	-
79-67240	N_2H_4	0.10	0.11	0.13	0.14	0.14
79-67240	UDMH	0.33	0.55	0.66	0.71	-
79-67240	A-50	0.09	0.16	0.19	0.21	0.22
79-67240	A-50*	0.13	0.21	0.23	0.29	0.29
56838	UDMH	No Activity				
50-67226	N_2H_4	0.03	0.09	0.12	0.14	0.16
50-67226	N_2H_4*	0.05	0.10	0.14	0.17	0.19
50-67226	UDMH	0.37	0.49	0.56	0.60	-
50-67226	A-50	0.03	0.09	0.13	0.15	0.16
50-67226	A-50*	0.05	0.11	0.15	0.18	0.18
70459-60	UDMH	0.45	0.51	0.56	0.61	0.64
70459-60	N_2H_4	0.15	0.24	0.26	0.30	0.31
70459-60	N_2H_4*	0.13	0.24	0.26	0.28	0.29
70459-60	A-50	0.16	0.19	0.20	0.21	0.22
70459-60	A-50*	0.20	0.27	0.29	0.31	0.32
70457-8	UDMH	0.52	0.62	0.68	-	-
70485-6	UDMH	0.58	0.63	0.71	-	-
70453-4	UDMH	0.52	0.64	0.70	-	-
73233-2a	UDMH	No Activity				
73233-1a	UDMH	0.36	0.58	0.87	-	-
71202-7	UDMH	No Activity				
71210-1	UDMH	No Activity				
75358	UDMH	0.42	0.60	0.70	-	-

*After one hour at 100 ma/cm².

3. Future Plans

A further effort will be made to find a good UDMH catalyst this next quarter. In the next month further noble metal alloys, precipitated Mo, Re, and oxide types will be fabricated into electrodes and will be tested. Once the catalyst system has been established and the electrode characteristics determined, 1/3 ft^2 electrodes will be designed, fabricated, and tested.

C. SUBTASK 3.3 DESIGN OF 1/3 FT^2 ELECTRODE HOLDERS

1. General Considerations

Major factors that must be considered in designing fuel cell electrode holders and manifolding are summarized in Table 21.

Table 21

FUEL CELL ELECTRODE HOLDER DESIGN FACTORS

Factor	Type
Sealing	Mechanical
Pressure Drop	Mechanical
Land to Groove Ratio	Mechanical-Electrical
Heat Transfer	Mechanical-Process
Water and Other Byproduct Removal	Process
Reactant Distribution and Concentration	Process
Cell Geometry	Mechanical
Current Collection	Electrical
Half-Cell Reaction	Process

While several of these factors are interrelated (e.g., land-to-groove ratio and current collection method affect both electrode support and internal electrical losses) the above listing

provides a convenient approach to the overall task. No order of importance has been attached to the various factors, primarily because of the interrelationships mentioned and the necessity for considering the effect of each factor variation on the other factors.

This contract calls for the design of gas electrodes to utilize the following reactants:

Fuels: H_2
H_2-rich reformed Aerozine-50
Aerozine-50

Oxidizers: O_2
O_2-rich reformed N_2O_4
N_2O_4

Until experiments carried on in other tasks more clearly establish the compositions of the catalytically reformed fuel and oxidizer streams, exact establishment of suitable electrode holders for such streams is not possible.

If purification of the reformed streams is required, to supply pure hydrogen and pure oxygen, electrode holders with suitable manifolding will be required. This is not considered to be a complex task, since the cleanness of the H_2-O_2 reaction (H_2O is the only material byproduct) and the necessity for "deadending" to conserve reactants dictates water removal via a route other than purge or recirculation of reactant if system simplicity is desired. For this reason electrode holder designs for N_2O_4 should be adequate for the H_2 or O_2 streams.

Direct utilization of Aerozine-50 in the fuel cell has not, as yet, been satisfactorily achieved. Hence, design of electrode holders for this service must await further electrode and catalyst developments.

N_2O_4 can be directly utilized at presently available electrodes and emphasis has therefore been placed on design of the required 1/3-ft^2 N_2O_4 electrode holders.

2. N_2O_4 Electrode Holder Design Considerations

a. Half-Cell Reaction

Electroreduction of N_2O_4 can occur through several routes but the predominant reaction appears to be:

$$NO_2 + 2H^+ + 2e^- \longrightarrow NO + H_2O \qquad (26)$$

Reactant and product rates based on the above reaction are given in Table 22 at various current densities (reaction rates) for a 1/3-ft^2 electrode area.

Table 22

STOICHIOMETRIC PRODUCT AND FEED RATES FOR ELECTRO-OXIDATION OF N_2O_4, NO_2 to NO (1/3-FT^2 ELECTRODE AREA)

Current Density, amp/ft^2	Current, amp	Stoich. NO_2 Rate, g/min/ electrode	Stoich. NO Product, g/min/ electrode	Stoich. H_2O Product Rate, g/min/ electrode
25	8.3	0.119	0.077	0.046
50	16.7	0.238	0.155	0.093
100	33.3	0.476	0.310	0.186
150	50	0.714	0.465	0.279
200	66.6	0.952	0.620	0.372

In practice, byproduct NO diffuses back through the electrode from the catalytically active sites to the bulk of the reactant stream, with a consequent dilution effect on the N_2O_4 (NO_2) concentration. H_2O formed can enter the electrolyte or back-diffuse to the reactant stream, depending on temperature and electrode properties. Where H_2O does go to the NO_2 stream, some reaction with the NO_2 undoubtedly occurs, although the exact extent of this reaction is uncertain. Its effect on cell performance is probably highly dependent on flow rate, diffusion of H_2O in the gas stream, and concentrations.

Previous experiments (Ref. 27) showed that little degradation of cathode potentials is caused by NO concentrations in the NO_2 feed stream, up to 50% NO. For preliminary design purposes, then, a NO_2-byproduct exit stream with a maximum NO_2 concentration of 50% will be assumed.

Water transport problems are discussed in a subsequent section of this report.

b. Cell Geometry (Overall Shape and Size)

Minimum weight, volume, and sealing perimeter usually can best be realized in a cell of circular cross-section. However, gas manifolding in a circular cell can be complicated where a continuous flow-through is required as in the case of NO_2 streams, and where definite and complex flow patterns are dictated by process considerations.

Table 23 describes cell overall geometry variations for circular, square, and rectangular shapes for 48-in.^{2} (1/3-ft^2) electrodes.

Minimum sealing perimeter can be obtained with the circular shape, while minimum gross cross-sectional area (proportional to cell volume) is obtained with the square shape. Both perimeter and area differences are admittedly small, but the potential savings in volume and possibly weight indicated by the lower gross area of the square geometry suggests such a shape as being preferable. Designer's choice, then, is for the square electrode geometry.

Table 23

POTENTIAL CELL OVERALL GEOMETRY VARIATIONS FOR 1/3-FT^2 ELECTRODES

Shape	Dimensional Description	Seal Perimeter, in.	Gross Area, in.^{2}
Circular	8.0 in. active dia. 1.5 in. dia. manifold hub 3/8 in. wide perimeter seal	27.4	60
Square	6.9 x 6.9 in. active area 3/8 in. wide perimeter seal	30.6	58.5
Rectangular	6 x 8 in. active area 3/8 in. wide perimeter seal	31.0	59.0
	5.35 x 9 in. active area 3/8 in. wide perimeter seal	31.7	59.5
	4.8 x 10 in. active area 3/8 in. wide perimeter seal	32.6	59.7
	4.0 x 12 in. active area 3/8 in. wide perimeter seal	35.0	60.5

c. Reactant Distribution and Concentration -- Land-to-Groove Ratio

As discussed under "Cell Reaction" above it appears certain that it will be necessary to purge a considerable portion of the NO_2 feed stream (possibly up to 50%) to prevent excessive cathode polarization caused by decreased NO_2 concentration and/or high NO byproduct concentrations.

A long NO_2 flow path is therefore indicated to cause maximum contact of the continuously degradating NO_2 stream with the electrode surface and obtain as high a NO_2 utilization as is possible. Multiple pass of the NO_2 stream will best produce this extended contact, but care must be taken to prevent excessive pressure drops with resulting areas of high static pressure sufficient to cause gross transfer of NO_2 through the permeable electrode. Further, reasonable distribution of "strong" and "weak" pass streams is required to insure relatively even current densities across the electrode surface.

The grooving geometry that appears to best meet the above requirements is illustrated in Figure 17.

Experience has shown that the MRD carbon cathode performs well with a 1/8-inch groove, 1/8-inch land support and distribution system. Polarization curves for small, unsupported half-cell electrodes and for 1/16 ft^2, 1/8-inch land-groove supported electrodes are essentially identical. Mechanically, wider grooves and/or narrower lands usually cause excessive extrusion of the MRD electrodes into the flow channel with higher possibility of eventual electrode rupture.

For the grooving detail shown in Figure 17, as applied to the 1/3-ft^2 square geometry electrode shape, an overall flow length of approximately 19 inches per parallel path is obtained. Width of the repeating element is 3/4 inch, requiring nine such elements for the 48-$in.^2$ square electrode. This configuration always places the weakest (No. 3) NO_2 concentration pass of each element adjacent to a strongest concentration (No. 1) pass except for the last element. A single pass from inlet to exhaust manifold at the end of the nine multi-pass repeating groove elements will eliminate the exception.

This flow pattern should provide a reasonably even distribution of NO_2 over the entire electrode area, though a slight overall NO_2 concentration gradient from inlet to exhaust manifold will inevitably exist.

Pressure drops in the 19-inch long, multi-pass, parallel paths should be slight (<0.5-in. H_2O gauge if gas flows result in Reynolds Numbers (N_{Re}) less than 100. Figure 18 illustrates pressure drops in MRC fuel cell designs as determined in test fixtures

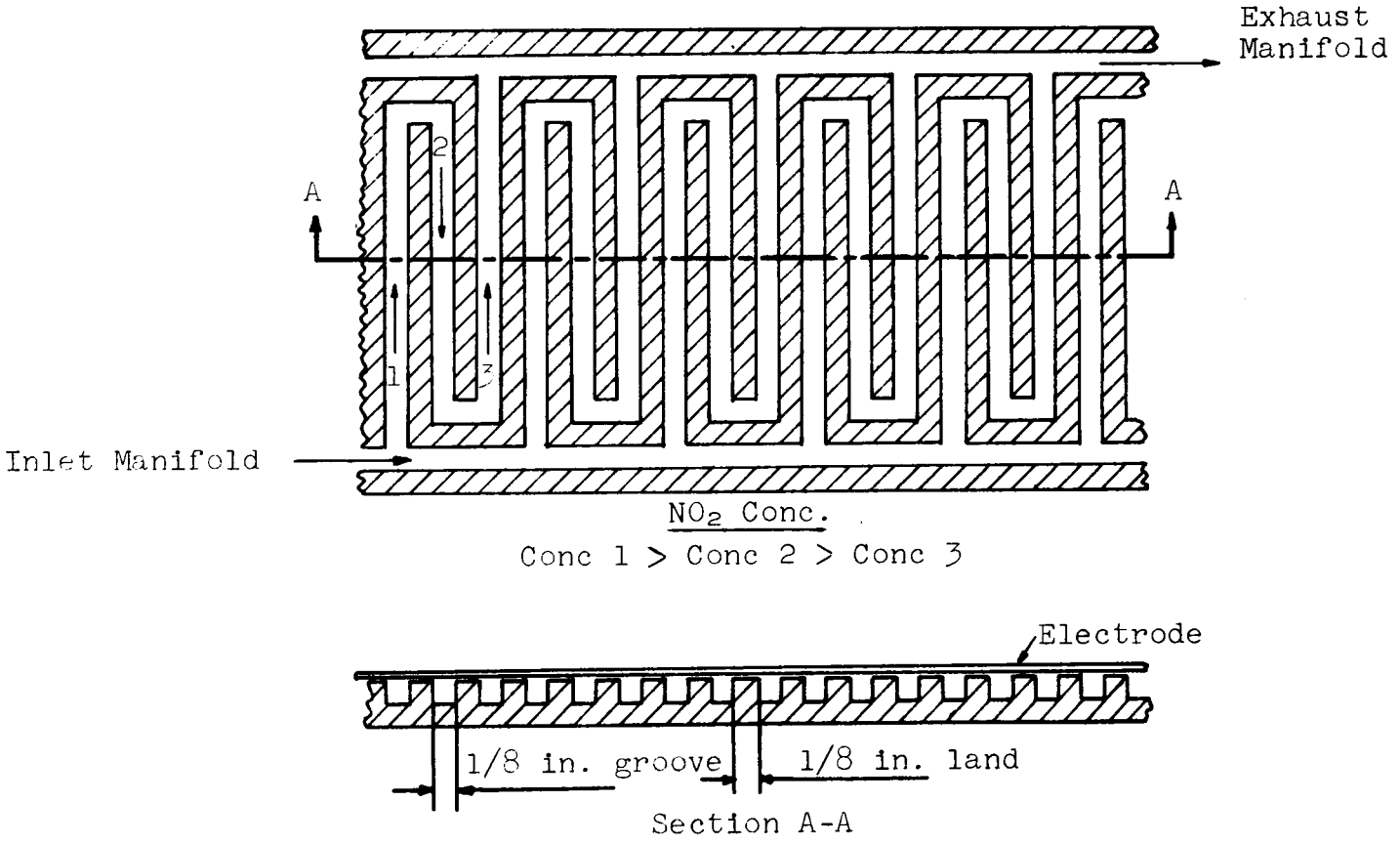

Figure 17. Grooving Detail

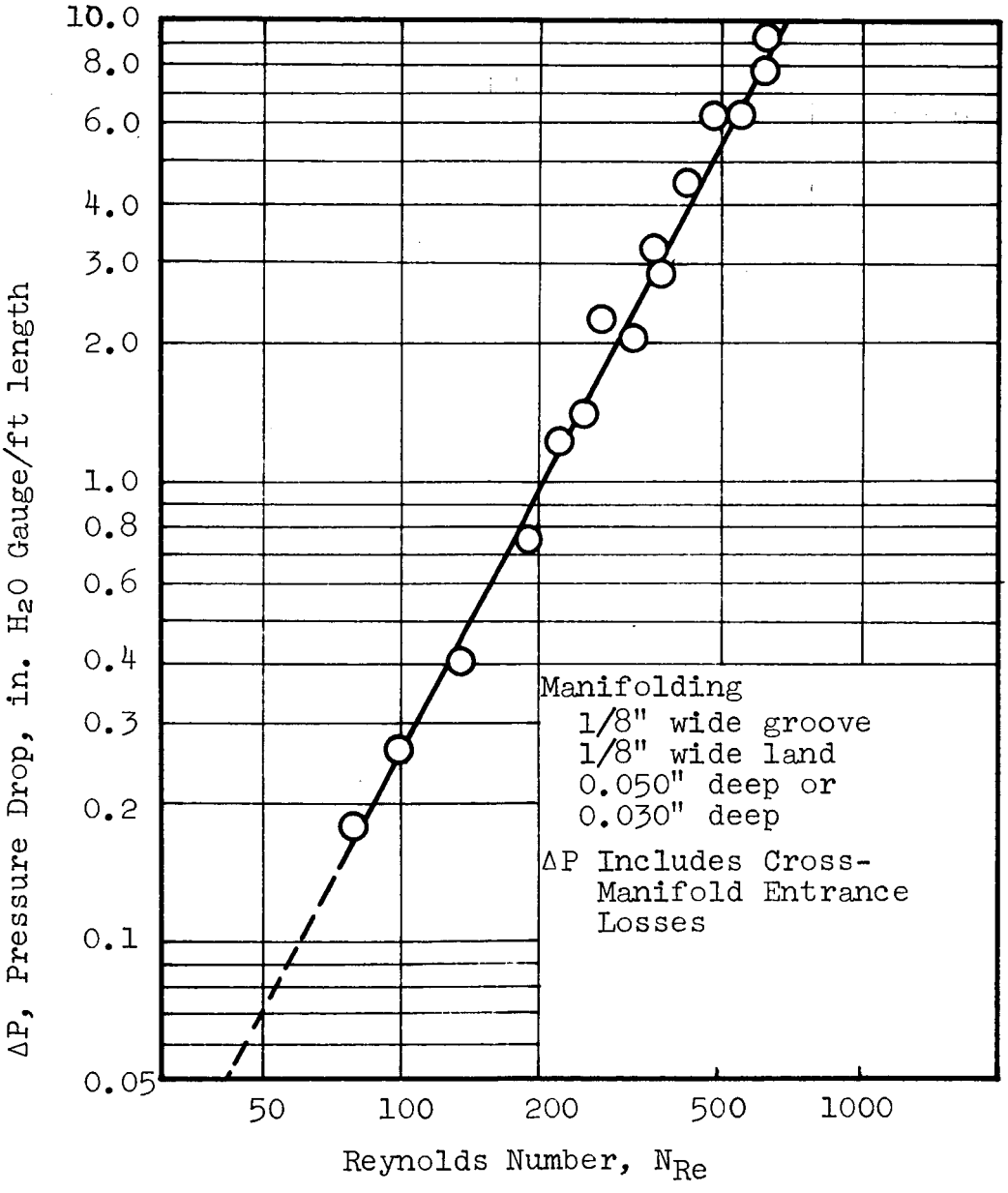

Figure 18. Pressure Drop in 1/8 in. Wide Gas Manifold Grooving; MRC Fuel Cell Designs

with 1/8-in. wide grooves on 1/4-in. centers, 0.050-in. or 0.030-in. deep grooves, with air as the test fluid.

From a mechanical standpoint, this multi-pass groove construction with 1/8-inch land, 1/8-inch groove will provide a land-to-groove ratio of approximately 0.7 when inlet and exhaust manifolds are considered. This value has been shown in previous proprietary work in our laboratory to provide adequate mechanical support with negligible internal electrical resistance losses due to contact area for current collection purposes at current densities up to at least 200 amp/ft^2.

d. Water Transport and Material Balance

It has been previously reported (Ref. 27 and 28) that the performance of MRD carbon cathodes is influenced to a considerable extent by N_2O_4 flow rates. A flow rate of 22 mg N_2O_4/min-cm^2 was found necessary for current densities in the range of 100 amp/ft^2. Such a flow rate represents a N_2O_4(NO_2) utilization efficiency of only about 8%. It was believed that the excessive N_2O_4 rates were necessary to remove back-diffused water of reaction, which tends to condense on the electrode surface due to transfer limitations. Such condensed water could block NO_2 diffusion to active sites either mechanically or through favoring of the reaction

$$3NO_2 + H_2O \longrightarrow 2HNO_3 + NO \text{ (warm concentrated solution)} \quad (27)$$

thus producing the more slowly diffusing HNO_3 as the active oxidant.

The flow rate of 22 mg N_2O_4/min-cm^2 corresponds to an average Reynolds Number

$$\frac{(\text{equiv dia})(\text{vel})(\text{density})}{\text{viscosity}} = N_{Re}$$

of approximately 40, which is still well within the laminar flow range and suggests H_2O transfer limitations due to poor film coefficients.

During the past period a further set of experiments was run to evaluate N_2O_4 cathode performance as a function of flow rate or average N_{Re}. Results are shown in Figure 19.

N_2O_4 flow rates were varied from approximately 10 to 30 mg N_2O_4/min-cm^2 so that N_{Re} varied over the relatively narrow laminar flow range of 25 to 70. Again, dependence of cathode potential on N_2O_4 flow (expressed as Reynolds Number) was shown to exist, particularly at the higher current densities.

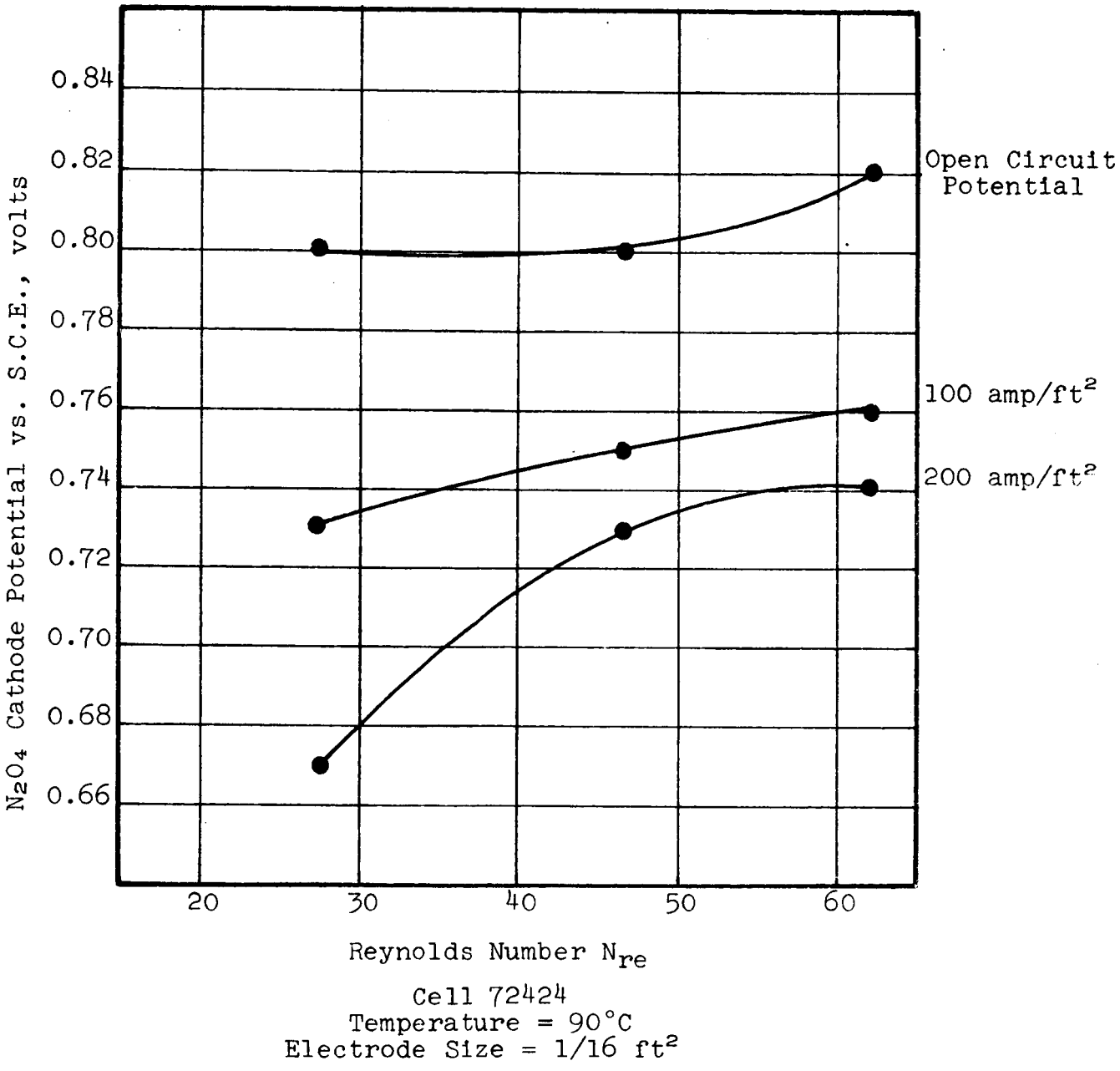

Figure 19. Effect of N_2O_4 Flow Rate (as Reynolds Number) on Cathode Polarization at Various Current Densities

It is not suggested that N_2O_4 cathode potential is solely a function of Reynolds Number, but it is apparent that flow, expressed as N_{Re} is an important factor, as evidenced by the relatively large potential variations seen in Figure 19 over a very small span of N_{Re}. It is concluded that, in general, Reynolds Numbers greater than about 50 should be maintained in grooving and manifolds of N_2O_4 cathodes.

A short experimental program to determine rate of water transfer through an MRD double, pressed, carbon cathode from a bulk liquid on one side to a flowing gas stream was undertaken.

An MRC carbon cathode, double thickness pressed together at 2660 psig, 25°C, was mounted between grooved end plates (1/8-in. land, 1/8-in. groove, 9-in.^{2} area). Water at various temperatures and ambient air at various flow rates were flowed on opposite sides of the electrode to vaporize H_2O from the liquid stream and cause diffusion through the cathode and into the gas carrier stream.

Humidity of the exit wet air was determined by wet bulb--dry bulb psychrometry, and checked by condensation of entrained water in a 0°C cold trap. Gas flow rates were determined with a precision rotameter calibrated with a wet test meter. Results are shown in Figure 20, which compares weight of water transferred through the electrode and removed by the gas stream in g H_2O/min/in.^{2} of electrode with an average calculated Reynolds Number evaluated at mean gas exit temperatures.

Data points were obtained only for the case where the gas stream was not saturated with water vapor. Thus at 70°C liquid temperature gas flows equivalent to a N_{Re} of less than about 200 result in a saturation condition. At the three temperatures evaluated, a limiting H_2O diffusion rate through the electrode was found, as shown by Figure 21.

For the case where a N_2O_4 flow of 22 mg/min-cm^2 was required it was found that operation at water balance dictates a carrier gas humidity of 0.027 g H_2O/g bone-dry gas. Since at the low N_{Re} encountered ($\approx$40) the gas stream was surely saturated ($\approx$0.15 g H_2O/g bone-dry gas) as shown by Figure 20, it can only be concluded that water removal far exceeded the water balance requirement and concentration effects as predicted by the Nernst equation probably contributed to the poor cathodic performance at low flow rates.

The MRD double pressed cathode permits H_2O vapor diffusion of about 0.065 g/min-in.^{2} at 90°C liquid temperature while water removed by gas humidification should be only about 0.0037 g/min-in.^{2} from stoichiometric considerations. It is concluded that greater diffusion control in the cathode is necessary.

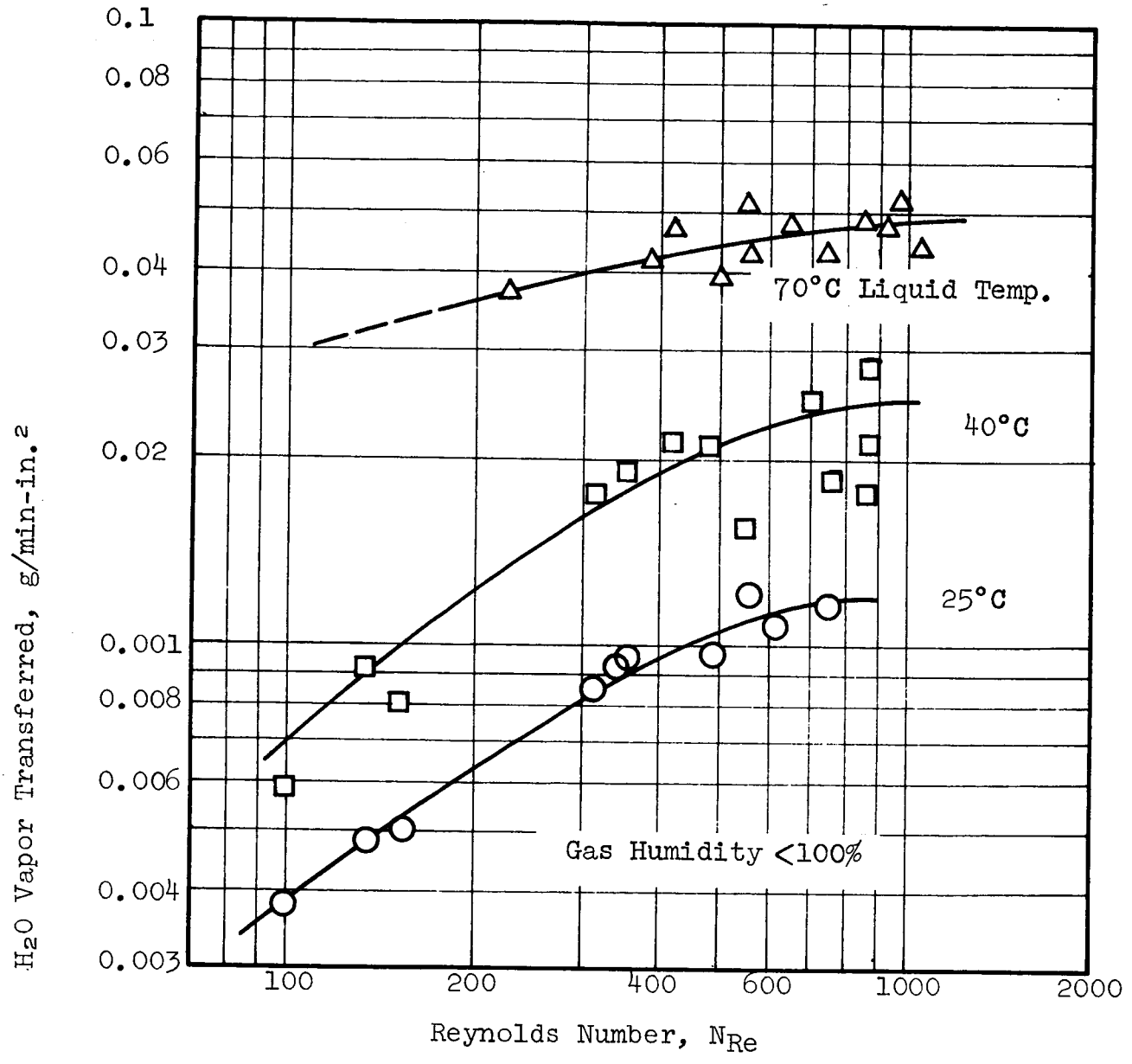

Figure 20. Water Transfer Characteristics of MRD Double Pressed Carbon Cathode

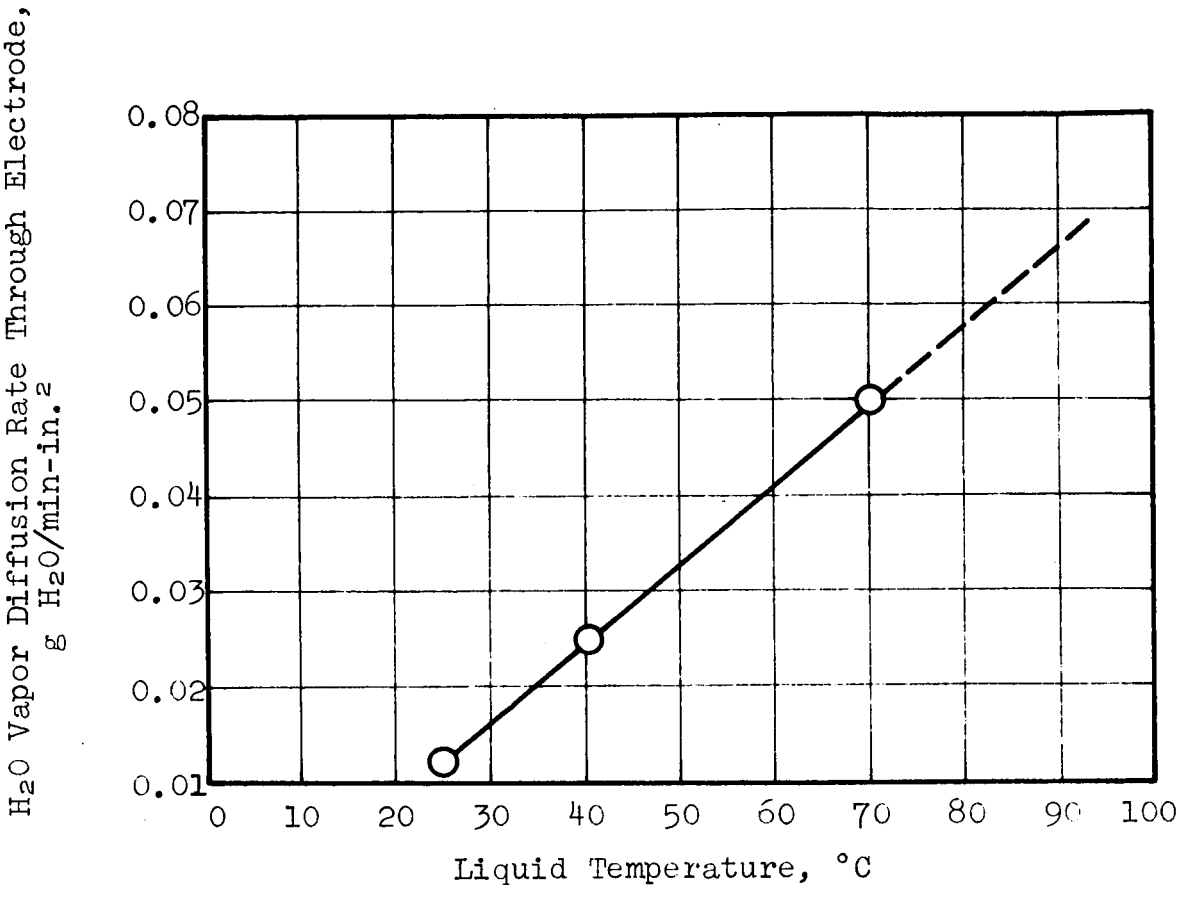

Figure 21. Water Vapor Diffusion Through MRD Double-Pressed Carbon Cathode

A material balance (Table 24) on a single 1/3-ft^2 N_2O_4 cathode at 100 ASF load indicates that an operating temperature of 70°C is required for water balance at a 1:1 NO, NO_2 mole ratio in the exit gas.

If NO_2 is completely consumed so that exit gas contains only NO and water, the water balance temperature is 81°C. These calculations assume no reaction between NO_2 and water vapor.

e. Proposed Test Cell Construction

A 1/3-ft^2 test cell design has been made to evaluate the grooving and flow arrangements previously discussed. A 7 x 7 in. active electrode area unit has been selected with construction similar to that of the 3 x 3 in. cells presently in use at MRC. Principal feature of the large size test cell is a replaceable flow plate permitting testing with various groove arrangements and depths.

Details of the frame and insert are shown in Figure 22. The center exposed electrode area is 7 x 7 in. Sealing between the electrode and frame is provided by a 0.25-in. wide 0.020-in. thick lip around the perimeter of the electrode. Insert to frame sealing is provided by an O-ring as shown. Reactant flow passages across the face of the electrode will be in the form of slots cut in a removable plate. The design of the initial flow plate is shown in Figure 23. Shown also in Figure 23 is the way in which the flow plate pattern will mate with the insert manifolds providing inlet and outlet for the pattern. Due to the replaceability of this flow plate, different flow patterns and groove depths may be accommodated by fabrication of additional plates.

f. Future Work

Construction of the proposed 1/3-ft^2 test cell is planned for the next quarter and an experimental program to evaluate electrochemical performance under varying process conditions will be executed.

Table 24

MATERIAL BALANCE ON 1/3-FT^2 N_2O_4 CATHODE AT 100 ASF

A. Assume exit gas contains NO_2 and NO in 1:1 mole ratio.

Component	Weight Rate In, g/min	Weight Rate Out, g/min
H	0.021	
NO_2	0.952	0.476
NO		0.31
H_2O		0.186
TOTALS	0.973	0.972

Average molecular weight of bone dry exit gas = 38.1

Actual humidity of exit gas at water balance is

0.186 g H_2O/0.786 g bone dry gas = 0.236

$$\text{Humidity} = \frac{mw_{H_2O}\ (p)}{mw_{\text{bone dry gas}}\ (1-p)}$$

where mw = molecular weight

p = partial pressure of water

$$0.236 = \frac{18\ (p)}{38.1\ (1-p)} \qquad p = 0.33 \text{ atm}$$

Corresponding to water vapor pressure at 70°C above 5M H_3PO_4.

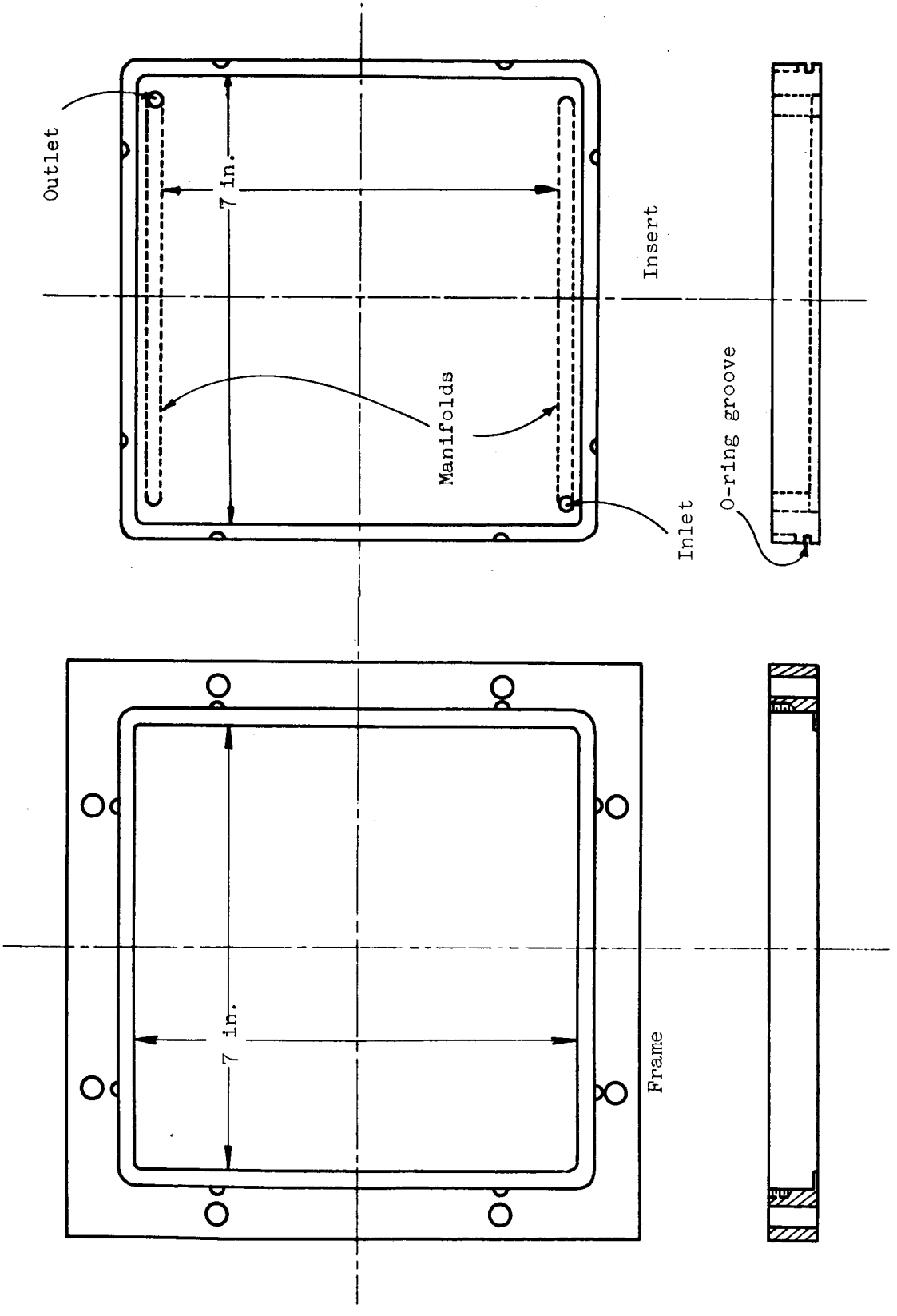

Figure 22. Proposed Test Cell Construction

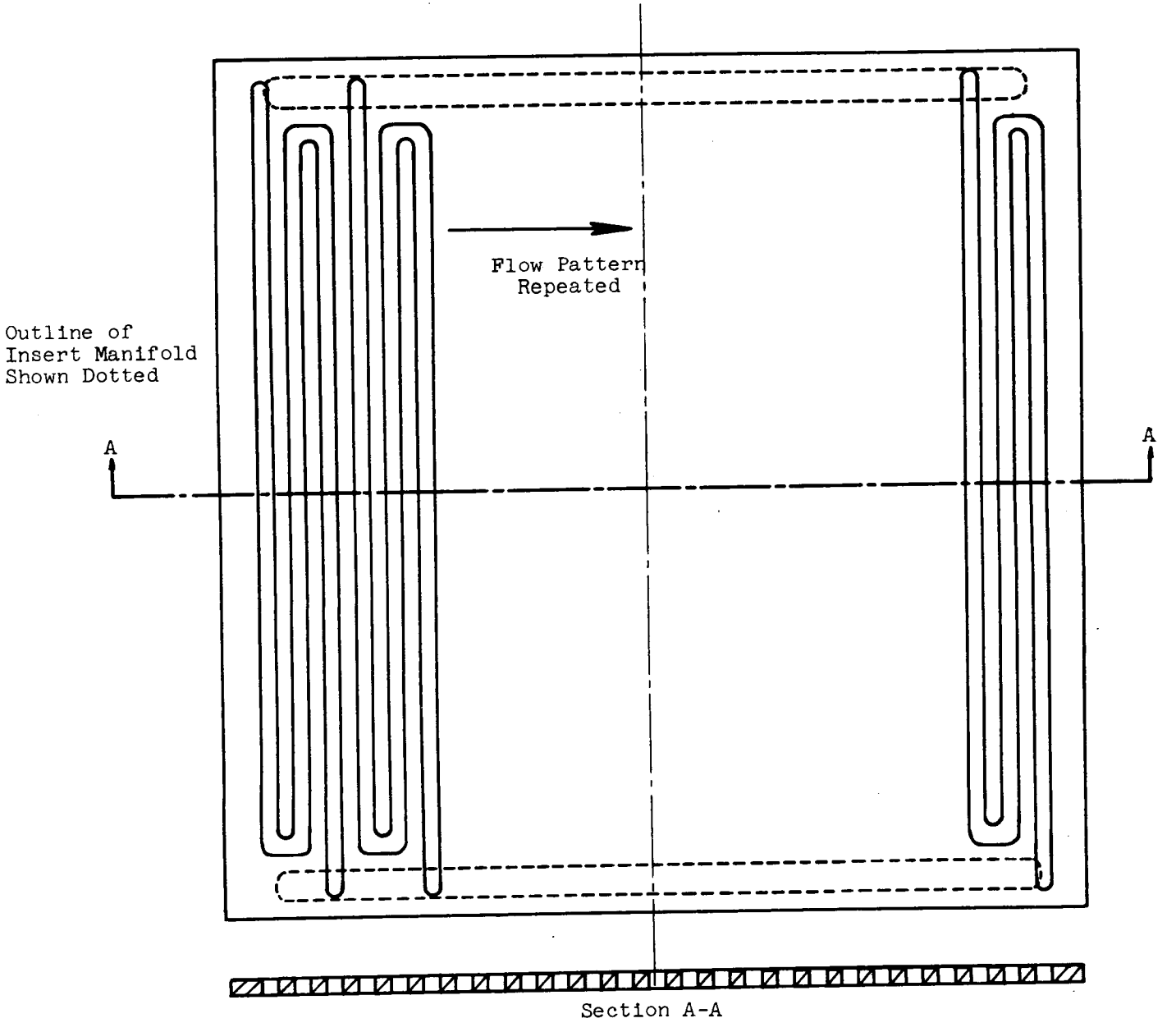

Figure 23. Reactant Flow Plate

V. REFERENCES

1. J. C. Orth, "Study of Fuel Cells Using Storable Rocket Propellants", Final Report Contract NAS3-4175, to be published.

2. L. F. Audrieth and W. L. Jolly, "Catalytic Decomposition of Highly Concentrated Hydrazine by Raney Nickel", J. Phys. and Colloid Chem., 55, 524-531 (1951).

3. N. P. Keier, G. K. Boreskov, V. V. Rode, A. P. Terent'ev, and E. G. Rukhadze, Kinetika i Kataliz, 2:4, 509-518 (1961).

4. German Patent 1108192, October 1959 to Engelhard Industries, Inc.

5. H. W. Lucien, "Thermal Decomposition of Hydrazine", J. Chem. Eng. Data, 6, 584 (1961).

6. T. J. Hanratty, J. N. Pattison, J. W. Clegg, and A. W. Lemmon, Jr., "Thermal Decomposition of Hydrazine Vapor in a Silica Vessel", Ind. Eng. Chem., 43, 1113 (1951).

7. U.S. Patent 900,453, "Catalytic Decomposition of 1,1-Dimethylhydrazine", July 4, 1962, to Engelhard Industries, Inc.

8. H. F. Cordes, "The Thermal Decomposition of 1,1-Dimethylhydrazine", J. Phys. Chem., 65, 1473-1477 (1961).

9. P. Gray and J. C. J. Thyme, "Kinetics of Hydrogen Abstraction from Hydrazine, Ammonia, and Trideuteroammonia", Trans. Faraday Soc., 60, 1047 (1964).

10. M. Szwarc, "The Dissociation Energy of the First N-H Bond in Ammonia", J. Chem. Phys. 17, 505 (1949).

11. M. Szwarc, "The Dissociation Energy of the C-N Bond in Benzylamine", Proc. Roy. Soc. (London), A198, 285 (1949).

12. I. J. Eberstein and I. Glassman, "Consideration of Hydrazine Decomposition", Progr. Astron. Rocketry, 2, 351 (1960).

13. K. A. Kobe and R. E. Pennington, "Thermochemistry for the Petrochemical Industry", Part XII, Petrol. Refiner, 29:7 (1950).

14. L. L. Wikstrom and K. Nobe, "Catalytic Decomposition of Nitrogen Dioxide", Ind. Eng. Chem., Process Design Develop., 4:2, 191 (1956).

15. S. Sourirajan and J. L. Blumenthal, "Catalytic Decomposition of Nitric Oxide Present in Low Concentrations; Actes Du Deuxieme Congres International De Catalyse, Tome II, Technip", Paris (1960).

16. F. Kaufman and J. R. Kelso, "Thermal Decomposition of Nitric Oxide", J. Chem. Phys., 23:9, 1702 (1955).

17. J. M. Fraser, F. Daniels, "The Heterogeneous Decomposition of Nitric Oxide with Oxide Catalysts", J. Phys. Chem., 62, 215 (1958).

18. J. C. Treacy and F. Daniels, "Kinetic Study of Oxidation of Nitric Oxide with Oxygen in the Pressure Range 1 to 20 mm", J. Am. Chem. Soc., 77:8, 2033 (1955).

19. C. H. Li, "Worksheet Gives Optimum Conditions", Chem. Eng., 65, 151 (1958).

20. M. S. Peters and J. L. Holman, "Vapor and Liquid Phase Reactions Between Nitrogen Dioxide and Water", Ind. Eng. Chem., 47:12, 2536 (1955).

21. K. G. Denbigh and A. J. Prince, "Kinetics of Nitrous Gas Absorption in Aqueous Nitric Acid", J. Chem. Soc., 1947, 790.

22. P. G. Caudle and K. G. Denbigh, "Kinetics of the Absorption of Nitrogen Peroxide into Water and Aqueous Solutions", Trans. Faraday Soc., 49, 39 (1953).

23. M. S. Peters, C. P. Ross, and J. E. Klein, "Controlling Mechanism in the Aqueous Absorption of Nitrogen Oxides", Am. Inst. Chem. Eng. J., 1, 105, (1955).

24. F. J. Welcher (ed), "Standard Methods of Chemical Analysis", Vol 2, Part A, 6th ed., Van Nostrand Company, Inc., Princeton, New Jersey, 562 (1963).

25. J. O. Smith, "Study of Fuel Cells Using Storable Rocket Propellants", Contract NAS3-2791, Final Report, NASA No. CR54116, 11 May 1964.

26. D. M. King and A. J. Bard, "The Electrochemistry of the Methylhydrazines", J. Am. Chem. Soc., 87:3, 419 (1965).

27. J. C. Orth, "Study of Fuel Cells Using Storable Rocket Propellants", 8th Monthly Report, Contract NAS3-4175, 10 January 1965.

28. Ibid., 7th Monthly Report, 10 December 1964.

APPENDIX I

WORK PLAN

PHASE I. PRELIMINARY TEST PROGRAM

TASK 1. AEROZINE-50 REFORMING STUDIES

A. OBJECTIVE

Determine the best catalysts and conditions for the reforming of Aerozine-50 to a hydrogen-rich feed stock suitable for fuel cells. Design, construct and operate (for 1000 hours)) a breadboard reformer.

B. BACKGROUND

The N_2H_4 component of Aerozine-50 decomposes readily to H_2 and N_2. The reforming of the UDMH fraction was demonstrated in the last contract and is the primary reactant in this work. Present plans are to use an available MRC reformer unit (well proven in hydrocarbon reforming) rather than rebuild the reformer used in the previous contract. Technical assistance in this work will be provided by Dr. B. M. Fabuss who has had 15 years' experience in related fields.

C. WORK PLANS

Subtask

1.1a Procure necessary parts and catalysts, and assemble high-temperature reformer.

1.1b Assemble low-temperature reactor.

1.2a,b Run initial screening tests.

(a) Eleven commercial catalysts were chosen of precious metal, nickel, and oxide types supported on activated alumina. They are known NH_3-dissociating or steam-reforming catalysts with several experimental catalysts included. Molecular sieve and activated carbon catalysts will be formulated and tested also.

(b) Screening runs will be made in both reactors. The feed stocks will be: UDMH alone, N_2H_4 alone, Aerozine 50 and H_2O, UDMH and H_2O. Product analysis will be made by appropriate traps (e.g.; H_2SO_4 solution for NH_3, KOH solution for CO_2, cold trap for liquid products) and VPC (H_2, CO, N_2, CH_4).

Subtask	
1.3	Completely characterize the best catalyst(s). The best catalyst(s) found in the screening runs will be completely characterized with respect to the operating parameters and their effect on product species and amount.
1.4	Design breadboard reformer using catalyst and conditions agreed upon with Project Monitor. Procure parts, construct equipment and perform initial testing and debugging., Set up control and safety instrumentation.
1.5	Test reformer for 1000 hours of continuous operation. Analyze product, 5 days/week.

TASK 2. N_2O_4 CATALYTIC DECOMPOSITION

A. OBJECTIVE

Determine the best catalysts and conditions for the decomposition of N_2O_4 into an oxygen-rich feed stock suitable for fuel cells. Design, construct, and operate (for 1000 hours) a breadboard reformer.

B. BACKGROUND

The reaction $N_2O_4 = 2NO + O_2$ goes essentially to completion without catalysts at 600°C; however, at room temperature the reaction is essentially complete in the reverse direction. One objective of this work is to promote this reaction at lower temperatures by proper manipulation of kinetic parameters.. The problem then is the decomposition of NO to its constituents in an oxygen-rich environment. Present plans are to modify a reformer unit to investigate these reactions.

C. WORK PLANS

Subtask	
2.1	Procure necessary parts and catalysts, and assemble reactor.
2.2	Run initial screening tests.

(a) Nine commercial catalysts were chosen of precious metal, nickel and copper oxides supported on activated alumina. Some are known nitrogen oxide decomposing catalysts. Several different substrates and catalyst types will be fabricated and tested.

(b) Screening runs will be made at temperatures between 200 and 800°C and several flow rates. Unconverted NO (or NO_2) will be allowed to convert back to N_2O_4 in a time column and subsequently will be removed in a cold trap. Product O_2 and N_2 will be determined.

Subtask

2.3 Completely characterize the best catalyst(s). The best catalyst(s) found in the screening runs will be completely characterized with respect to the operating parameters (including pressure) and their effect on the amount of NO converted.

2.4 Design breadboard reformer using catalyst and conditions agreed upon with Project Monitor. Procure parts, construct equipment, perform initial testing and debugging. Set up control and safety instrumentation.

2.5 Test reformer for 1000 hours of continuous operation. Analyze product, 5 days/week.

TASK 3. ELECTRODE DEVELOPMENT - DIRECT REACTANT USE

A. OBJECTIVE

Develop electrodes capable of operating on Aerozine-50 and N_2O_4 directly with maximum efficiency on a single pass through the electrode chamber. Design, construct, and characterize electrodes and holders of 1/3 ft^2 size.

B. BACKGROUND

Work on the previous contracts has produced semioptimized electrodes for both N_2O_4 and N_2H_4. Continuation of this work is necessary in order to adapt the anode for Aerozine-50 and to improve N_2O_4 utilization efficiency. Electrode design work is required to meet the new requirements for maximum utilization in a single pass of reactant.

C. WORK PLANS

Subtask

3.1 Cathode optimization studies.

(a) Statistical optimization study of electrode manufacturing procedures, carbon type, catalysts, porosity.

(b) Complete characterization of best combination of factors found above in prototype electrodes and cells.

3.2 Development of Aerozine-50 anode.

(a) Adapt MRD-A platinum-Teflon anode for use on liquid and/or vapor N_2H_4. Main problem: develop a diffusion barrier to prevent decomposition of N_2H_4 prior to electro-oxidation.

Subtask

3.2 (b) Test electrode developed above with Aerozine-50. Determine and test other catalysts which might oxidize methyl-hydrazines more efficiently.

(c) Complete characterization of best combination of factors found above in prototype electrodes and cells.

3.3 Design 1/3-ft^2 electrodes and test cells. Present plans for improving reactant utilization on a single pass involve designing the electrodes to give the highest possible reactant contact time to the electrode. This can be accomplished by the incorporation of baffles in the electrode chamber and by adjustment of the electrode and manifold geometry to yield high Reynolds Numbers for the gas flow. Water balance and reactant efficiencies are part of the considerations involved.

3.4 Electrode Tests.

Based on the results of the design studies several electrode and half-cell modifications will be constructed and experiments conducted to determine flow patterns, residence time, pressure drop, Reynolds Numbers, etc. From this work the physical factors important to good electrode performance will be elucidated and optimized.

3.5,3.6 To determine coulombic efficiencies, material balance calculations will require analytical methods to determine relative amounts of reactants and products for both electrodes. When possible standard methods will be used; otherwise methods will be developed and proven.

3.7,3.8 The final design of the 1/3 $ft.^2$ electrode and holder for the N_2O_4 cathode will be fully characterized in half cells using H_2 counter electrodes and acid electrolytes. Similarly the Aerozine-50 anode will be fully characterized using O_2 counter electrodes and acid electrolyte. Included in the characterization will be performance, coulombic and voltage efficiency at 6, 12, and 24 watts. Open-circuit tests will be made with flowing reactant streams to determine the amount of self decomposition.

APPENDIX II

CATALYST DATA

Type Number: G-43 Manufacturer: Girdler

Classification: Reduction of Nitrogen Oxides

Temperature Range: Not specified

Active Material: Platinum Promoted

Substrate or Support:

Size: 1/4"x 1/4" Shape: Tablets

Additional Information: Highly active, physically rugged. Presently in commercial use in petrochemical industry.

Type Number: T-1144 Manufacturer: Girdler

Classification: Experimental

Temperature Range:

Active Material: Nickel Oxide 50% Nickel

Substrate or Support: Refractory Oxide

Size: 3/16"x 1/8" Shape: Tablets

Additional Information:

Type Number: T-310 Manufacturer: Girdler

Classification: Experimental

Temperature Range: Not specified

Active Material: Nickel Oxide 10-12% nickel

Substrate or Support: Activated Alumina

Size: 3/16" x 1/8" Shape: Tablets

Additional Information:

Type Number: T-366 Manufacturer: Girdler

Classification: Experimental

Temperature Range: Not Specified

Active Material: Copper 50%

Substrate or Support: Kieselguhr

Size: Powder Shape:

Additional Information: Stabilized to be non-Pyrophoric.

Type Number: T-317 Manufacturer: Girdler

Classification: Experimental

Temperature Range: Not Specified

Active Material: Copper Oxide 10-12%

Substrate or Support: Activated Alumina

Size: 3/16" x 1/8" Shape: Tablets

Additional Information:

Type Number: T-315 Manufacturer: Girdler

Classification: Experimental

Temperature Range: Not Specified

Active Material: Copper Oxide (3 to 4%)

Substrate or Support: Activated Alumina

Size: 3/16" x 1/8" Shape: Tablets

Additional Information: Active material concentrated in thin outer layer.

Type Number: T-313 Manufacturer: Girdler

Classification: Experimental

Temperature Range: Not Specified

Active Material: Nickel 3-4%, Copper 0.2%

Substrate or Support: Activated Alumina

Size: 3/16" x 1/8" Shape: Tablets

Additional Information: Active materials concentrated in thin outer layer.

Type Number: G-31 Manufacturer: Girdler

Classification: Steam Reforming

Temperature Range: 950°-1150°C

Active Material: Nickel

Substrate or Support: Alumina

Size: 5/8" to 1-1/2 Shape: Lump

Additional Information: High activity may have to be crushed for trials.

Type Number: ICI-35-4 Manufacturer: Girdler

Classification: Ammonia Synthesis

Temperature Range: Not Specified

Active Material: Triple Promoted Iron Oxide

Substrate or Support:

Size: 2-8 mm Shape: Granules

Additional Information: Long life - High or low temperature operation - Poisoned by sulfur or oxygen compounds.

Type Number: G-56 Manufacturer: Girdler

Classification: Ammonia Dissociation and Steam Reforming

Temperature Range: Not Specified

Active Material: Nickel

Substrate or Support:

Size: 5/8 x 3/8 Shape: Raschig Rings

Additional Information:

Type Number: G-29 Manufacturer: Girdler

Classification: Ammonia Dissociation

Temperature Range: Not Specified

Active Material: Nickel

Substrate or Support:

Size: 1/2" Shape: Cylinders

Additional Information: Also used for steam reforming.

Type Number: G-47 Manufacturer: Girdler

Classification: Ammonia Dissociation

Temperature Range: 850°-980°C

Active Material: Iron Oxide

Substrate or Support:

Size: 1/4" Shape: Spheres

Additional Information: High spare velocities.

Type Number: MRC-MnO_2 Manufacturer: MRC

Classification: Experimental

Temperature Range: 100-500°C

Active Material: MnO_2

Substrate or Support:

Size: Shape:

Additional Information:

Type Number: 3355 Manufacturer: Engelhard

Classification:

Temperature Range:

Active Material: 0.5% Platinum

Substrate or Support: Alumina

Size: 1/8" Shape: Pellets

Additional Information:

Type Number: 4747 Manufacturer: Engelhard

Classification:

Temperature Range:

Active Material: 0.5% Rhodium

Substrate or Support: Alumina

Size: 1/8" Shape: Pellets

Additional Information:

Type Number: 3352 Manufacturer: Baker Div.-Engelhard

Classification:

Temperature Range:

Active Material: 0.5% Platinum

Substrate or Support: Alumina

Size: 1/8" Shape: Pellets

Additional Information:

Type Number: 3054 Manufacturer: Baker Div.-Engelhard
Classification:
Temperature Range:
Active Material: 0.5% Ruthenium
Substrate or Support: Alumina
Size: 1/8" Shape: Pellets
Additional Information:

Type Number: 3107 Manufacturer: Baker Div.-Engelhard
Classification: Hydrogenation
Temperature Range: Not Stated
Active Material: 0.5% Palladium
Substrate or Support: Alumina
Size: 1/8" Shape: Pellets
Additional Information: Experimental

Type Number: T-312 Manufacturer: Girdler

Classification: Experimental

Temperature Range: n/s

Active Material: Nickel and Copper Oxides

Substrate or Support: Activated Alumina

Size: 3/16" x 1/8" Shape: Tablets

Additional Information: Carrier - alumina containing 10-12% nickel and 1% copper.

Type Number: 309 Manufacturer: Girdler

Classification: Experimental

Temperature Range: n/s

Active Material: Platinum Oxide

Substrate or Support: Alumina

Size: 3/16" x 1/8" Shape: Tablets

Additional Information: Platinum Oxide concentrated in thin outer layers on active alumina substrate containing 0.1% platinum.

DISTRIBUTION LIST

Contract No. NAS3-6476 MRB5009Q1

National Aeronautics and Space Administration
Washington, D. C. 20546
Attention: Ernst M. Cohn, Code RNW
George F. Esenwein, Code MAT
J. R. Miles, Code SL
A. M. Andrus, Code ST

National Aeronautics and Space Administration
Goddard Space Flight Center
Greenbelt, Maryland 20771
Attention: Thomas Hennigan, Code 632.2

National Aeronautics and Space Administration
Lewis Research Center
21000 Brookpark Road
Cleveland, Ohio 44135
Attention: B. Lubarsky, M.S. 500-201
R. L. Cummings, M.S. 500-201
H. J. Schwartz, M.S. 500-201
J. E. Dilley, M.S. 500-309
N. D. Sanders, M.S. 302-1
M. J. Saari, M.S. 500-202
R. R. Miller, M.S. 500-202
Technology Utilization Office, M.S. 3-16
R. B. King, M.S. 500-201 (1 copy + 1 reproducible)
Library, M.S. 3-7
Report Control, M.S. 5-5
V. F. Hlavin, M.S. 3-14

National Aeronautics and Space Administration
Western Operations Office
Santa Monica, California 90406
Attention: P. Pomerantz

Jet Propulsion Laboratory
4800 Oak Grove Drive
Pasadena, California 91103
Attention: Aiji Uchiyama

U. S. Army Electronics R and D Labs
Fort Monmouth, New Jersey
Attention: Arthur F. Daniel (Code SELRA/SL-PS)
Dr. H. F. Hunger (Code SELRA/SL-PS)
David Linden (Code SELRA/SL-PS)
Dr. Adolph Fischbach

U. S. Army Research Office
Physical Sciences Division
3045 Columbia Pike
Arlington, Virginia

Western Reserve University
Cleveland, Ohio
Attention: Prof. Ernest Yeager

National Aeronautics and Space Administration
Scientific and Technical Information Facility
P. O. Box 5700
Bethesda, Maryland 20014
(2 copies + 1 reproducible)

National Aeronautics and Space Administration
Langley Research Center
Langley Station
Hampton, Virginia 23365
Attention: S. T. Peterson

National Aeronautics and Space Administration
Marshall Space Flight Center
Huntsville, Alabama 35812
Attention: Philip Youngblood
R. Boehme

National Aeronautics and Space Administration
Ames Research Center
Moffett Field, California 94035
Attention: James R. Swain, Pioneer Project
T. Wydeven, Environmental Control Branch
Jon Rubenzer, Biosatellite Project

National Aeronautics and Space Administration
Manned Spacecraft Center
Houston, Texas 77058
Attention: Richard Ferguson (EP-5)
Robert Cohen, Gemini Project Office
F. E. Eastman (EE-4)

U. S. Army Engineer R and D Labs
Fort Belvoir, Virginia 22060
Attention: Dr. Galen Frysinger (Code SMOFB-EP)
Electrical Power Branch

Research Office
R and D Directorate
Army Weapons Command
Rock Island, Illinois
Attention: Mr. G. Riensmith, Chief

U. S. Army Research Office
Chief, R and D
Department of the Army
3D442, The Pentagon
Washington, D. C. 20546
Attention: Dr. Sidney J. Mangram

Westinghouse Electric Corporation
Research and Development Center
Churchill Borough
Pittsburgh, Pennsylvania
Attention: Dr. A. Langer

Harry Diamond Labs.
Room 300, Building 92
Connecticut Avenue and Van Ness St.,N.W.
Washington, D. C.
Attention: Nathan Kaplan

Natick Labs.
Clothing and Organic Materials Division
Natick, Massachusetts
Attention: Leo A. Spano
Robert N. Walsh

U. S. Army Mobility Command
Research Division
Center Line, Michigan 48090
Attention: O. Renius (AMSMO-RR)

Office of Naval Research
Department of the Navy
Washington 25, D. C.
Attention: Dr. Ralph Roberts, Code 429
Head, Power Branch
H. W. Fox, Code 425

U. S. Naval Research Laboratory
Washington, D. C. 20390
Attention: Dr. J. C. White, Code 6160

Naval Ordnance Laboratory
Department of the Navy
Silver Spring, Maryland
Attention: Philip B. Cole, Code WB

Flight Vehicle Power Branch
Air Force Aero Propulsion Laboratory
Wright-Patterson Air Force Base, Ohio
Attention: J. E. Cooper, Code APIP

AF Cambridge Research Lab.
L. C. Hanscom Field
Bedford, Massachusetts
Attention: CRZE
Francis X. Doherty
Edward Raskind, Wing F

Office, DDR&E: USW & BSS
The Pentagon
Washington 25, D. C.
Attention: G. B. Wareham

Institute for Defense Analyses
Research & Engineering Support Division
400 Army-Navy Drive
Arlington, Virginia 22202
Attention: R. Hamilton
Dr. George C. Szego

Office of Technical Services
Department of Commerce
Washington, D. C. 20009

Army Materiel Command
Research Division
AMCRD-RSCM T-7
Washington 25, D. C.
Attention: John W. Crellin

U. S. Army Research Office
Box CM, Duke Station
Durham, North Carolina
Attention: Paul Greer
Dr. Wilhelm Jorgensen

Hq., U. S. Army Materiel Command
Development Division
Washington 25, D. C.
Attention: Marshall D. Aiken (AMCR-DE-MC-P)

Bureau of Naval Weapons
Department of the Navy
Washington 25, D. C.
Attention: Milton Knight, Code RAAE-50
Whitwell T. Beatson,
Code RAAE-52

Bureau of Ships
Department of the Navy
Washington 25, D. C.
Attention: Bernard B. Rosenbaum, Code 340
C. F. Viglotti, Code 660

Naval Ordnance Laboratory
Department of the Navy
Corona, California
Attention: William C. Spindler, Code 441

Space Systems Division
Los Angeles Air Force Station
Los Angeles, California 90045
Attention: SSSD

Rome Air Development Center, RSD
Griffiss AFB, New York 13442
Attention: Frank J. Mollura, RASSM

Army Reactors, DRD
U. S. Atomic Energy Commission
Washington 25, D. C.
Attention: D. B. Hoatson

Staff Metallurgist
Office, Director of Metallurgy Research
Bureau of Mines
Interior Building
Washington, D. C. 20240
Attention: Kenneth S. Higbie

Power Information Center
University of Pennsylvania
Moore School Building
200 South 33rd Street
Philadelphia 4, Pennsylvania

DISTRIBUTION LIST (Continued)

Contract No. NAS3-6476 MRB5009Q1

Aeronutronic Division
Philco Corporation
Ford Road
Newport Beach, California 92663
Attention: Dr. S. W. Weller

Allison Division
General Motors Corporation
Indianapolis 6, Indiana
Attention: Dr. Robert B. Henderson

Arthur D. Little, Inc.
Acorn Park
Cambridge, Massachusetts 02140
Attention: Dr. Ellery W. Stone

Atomics International,
Division of North American Aviation, Inc.
Canoga Park, California
Attention: Dr. H. L. Recht

Battelle Memorial Institute
505 King Avenue
Columbus, Ohio 43201
Attention: Dr. C. L. Faust

Electrochimica Corporation
1140 O'Brien Drive
Menlo Park, California
Attention: Dr. Morris Eisenberg

Electro-Optical Systems, Inc.
300 North Halstead Street
Pasadena, California
Attention: E. Findl

Esso Research & Engineering Company
Products Research Division
P. O. Box 121
Linden, New Jersey
Attention: Mr. Robert Epperly

General Electric Company
Direct Energy Conversion Operations
Lynn, Massachusetts
Attention: Dr. H. Maget

General Electric Company
Research Laboratory
Schenectady, New York
Attention: Dr. H. Liebhafsky

General Motors Corporation
Box T
Santa Barbara, California
Attention: Dr. C. R. Russell

G. M. Defense Research Lab.
P. O. Box T
Santa Barbara, California
Attention: Dr. Smatko

Alfred University
Alfred, New York
Attention: Prof. T. J. Gray

Allis-Chalmers Mfg. Company
1100 South 70th Street
Milwaukee, Wisconsin 53201
Attention: John Platner

American Machine and Foundry
689 Hope Street
Springdale, Connecticut
Attention: Dr. L. H. Shaffer, Research,
& Development Division

Astropower, Incorporated
Douglas Aircraft Company, Inc.
2121 College Drive
Newport Beach, California
Attention: Dr. Carl Berger

Bell Telephone Laboratories, Inc.
Murray Hill, New Jersey
Attention: Mr. U. B. Thomas

Clevite Corporation
Mechanical Research Division
540 East 105th Street
Cleveland, Ohio 44108
Attention: A. D. Schwope

Engelhard Industries, Inc.
497 Delancy Street
Newark 5, New Jersey
Attention: Dr. J. G. Cohn

The Franklin Institute
Benjamin Franklin Avenue at 20th Street
Philadelphia 3, Pennsylvania
Attention: Robert Goodman

Garrett Corporation 16
1625 Eye Street, N.W.
Washington 6, D. C.
Attention: George R. Sheperd

General Electric Company
Missile & Space Vehicle Department
P. O. Box 8555
Philadelphia, Pennsylvania 19101
Attention: E. W. Kipp, Room T-2513

General Motors Corporation
Research Laboratories
Electrochemistry Department
12 Mile & Mound Roads
Warren, Michigan 48090
Attention: Mr. Seward Beacom

Hughes Research Laboratories Corp.
Malibu, California
Attention: T. M. Hahn

DISTRIBUTION LIST (Continued)

Contract No. NAS3-6476 MRB5009Q1

Globe-Union, Inc.
900 East Keefe Avenue
Milwaukee, Wisconsin 53201
Attention: Dr. W. Towle

Ionics, Incorporated
152 Sixth Street
Cambridge, Massachusetts 02142
Attention: Dr. Werner Glass

Leesona Moos Laboratories
Lake Success Park
Community Drive
Great Neck, New York
Attention: Dr. A. Moos

Monsanto Research Corporation
Everett, Massachusetts 02149
Attention: Dr. J. Smith

Power Sources Division
Whittaker Corporation
9601 Canoga Avenue
Chatsworth, California 91311
Attention: Dr. M. Shaw

Radio Corporation of America
Astro Division
Heightstown, New Jersey
Attention: Dr. Seymour Winkler

Space Technology Laboratories, Inc.
2400 E. El Segundo Boulevard
El Segundo, California
Attention: Dr. A. Krauz

Stanford Research Institute
820 Mission Street
South Pasadena, California
Attention: Dr. Fritz Kalhammer

Thiokol Chemical Corporation
Reaction Motors Division
Denville, New Jersey
Attention: Dr. D. J. Mann

Tyco Laboratories, Inc.
Bear Hill
Waltham 54, Massachusetts
Attention: W. W. Burnett

University of Pennsylvania
Philadelphia, Pennsylvania 19104
Attention: Dr. Manfred Altman

Union Carbide Corporation
12900 Snow Road
Parma, Ohio
Attention: Dr. George E. Evans

The Western Company
Suite 802, RCA Building
Washington, D. C.
Attention: R. T. Fiske

Institute of Gas Technology
State and 34th Streets
Chicago, Illinois
Attention: Mr. Bernard Baker

Johns Hopkins University
Applied Physics Laboratory
8621 Georgia Avenue
Silver Spring, Maryland
Attention: W. A. Tynan

Midwest Research Institute
425 Volker Boulevard
Kansas City 10, Missouri
Attention: Dr. B. W. Beadle

North American Aviation, Inc.
S&ID Division
Downey, California
Attention: Dr. James Nash

Pratt & Whitney Aircraft Division
United Aircraft Corporation
East Hartford 8, Connecticut
Attention: Librarian

Rocketdyne
6633 Canoga Avenue
Canoga Park, California
Attention: Library, Dept. 586-306

Speer Carbon Company
Research and Development Laboratories
Packard Road at 47th Street
Niagara Falls, New York
Attention: Dr. L. M. Liggett

Texas Instruments, Inc.
13500 North Central Expressway
Dallas, Texas
Attention: Mr. Isaac Trechtenberg

Thomson Ramo Wooldridge, Inc.
23555 Euclid Avenue
Cleveland, Ohio 44117
Attention: Librarian

University of Pennsylvania
Philadelphia, Pennsylvania 19104
Attention: Prof. John O'M Bockris

Unified Science Associates, Inc.
826 South Arroyo Parkway
Pasadena, California
Attention: Dr. Sam Naiditch

University of California
Space Science Laboratory
Berkeley 4, California
Attention: Prof. Charles W. Tobias

Yardney Electric Corporation
40-50 Leonard Street
New York, New York
Attention: Dr. Paul Howard